ADDIS ABABA UNIVERSITY

ADDIS ABABA INSTITUTE OF TECHNOLOGY

SCHOOL OF MULTIDISCIPLINARY ENGINEERING

CENTER FOR MATERIALS ENGINEERING

A STUDY ON OPTICAL QUALITY ENHANCEMENT OF ALPHA-ALUMINA/TITANIA PEARLESCENT PIGMENT VIA INSITU pH CONTROL

BY: Buziye Guye

A Thesis Submitted to Addis Ababa Institute of Technology in Partial Fulfillment of the Requirement for the Degree of Masters of Science Materials Engineering

Addis Ababa, Ethiopia

October 2023

Addis Ababa University

Addis Ababa Institute of Technology

School of Multidisciplinary Engineering

Center for Materials Engineering

This is to certify that the thesis entitled "**A Study on Optical Quality Enhancement of Alpha-Alumina/Titania Pearlescent Pigment via Insitu pH Control**" and submitted in partial fulfillment of the requirements for the degree of Masters of Science (**Materials Engineering**) that complies with the regulations of the university and meets with the standard quality.

Approved by Examining Board:

Dr. Georgies Alene		Dec, 11, 2023
Head of School of Materials Engineering	Signature	Date
Dr. Anteneh Marelign		12/11/2023
Advisor	Signature	Date
Dr. Shimelis Shumi		13/11/23
Internal Examiner	Signature	Date
Dr. Shimelis Kebede		13/11/23
External Examiner	Signature	Date

DECLARATION OF ORIGINALITY

I, the researchers, confirm that the senior thesis titled on **"A Study on Optical Quality Enhancement of Alpha-Alumina/Titania Pearlescent Pigment via Insitu pH Control**" has not been submitted in any form for another degree, diploma or an award at any university or other institution of the tertiary education. My original work is being submitted at Addis Ababa Institute of Technology **University** in partial fulfillment for the award of an **MSc** degree in Materials Engineering. The work was under the guidance of Dr. Anteneh Marelign. Instructor in Addis Ababa University, School of Multidisciplinary Engineering Center for Materials Engineering.

Buziye Guye _____ _____

Student Name Signature Date

ACKNOWLEDGEMENT

First, I would like to thank the Almighty God for giving me the strength, patience and wisdom to overcome all the challenges I faced and for his protection and help at every step of my life and success in my work.

I would like to express my deepest and sincere gratitude to my advisor **Dr. Anteneh M.** Not only for spending his precious time reading every portion of the paper but also for his valuable comments, suggestion, invaluable supervision, inexpressible support, criticism throughout the research and continuous guidance without which it could have been impossible to complete this thesis work. His unlimited encouragements, motivation and suggestions have been always a source of inspiration and energy for me. He was much more than an advisor for me.

I would like to thank the managers and worker of leather and leather product research and development center of Ethiopia, Korea Advanced institute of Science and Technology **(KAIST)** central research laboratory, Bahirdar University and Addis Ababa Science and Technology University for their greater support for giving the information and chemical lab needed during the study and support to fill the research work.

Finally, I would like to thank my beloved family for their financial support and valuable morals until the study has been finished.

ABSTRACT

Pigment is a material that changes the color of reflected or transmitted light as the result of wavelength- picky immersion. During high-temperature calcination, there is a problem with the thermal expansion coefficient mismatch between mica and titania and the resulting thermal stress and crack formation. Thermal stress and crack formation is an issue during high-temperature calcination. Formation of cracks in the coating layer results in the scattering of light and the consequent decline of pearl luster. Various researchers have conducted a study on the low temperature rutile phase formation; however, the attempts have resulted in higher rutile phase fraction on the final coating but in most cases with compromised optical quality. In this study, α-Al_2O_3 platelets of average particle size ~ 10μm have been synthesized to be used as a substrate for the pearlescent pigment. Coating of TiO_2 on the surface of the synthesized α-Al_2O_3 was performed via co-precipitation method. Urea was utilized as a hydrolyzing and pH-regulating agent along with $TiOSO_4$ as a precursor to TiO_2The sample with lower oxysulfate:urea ratio (i.e. strongly acidic synthesis media) resulted in higher rutile phase fraction (41.5%) while the other two samples, where the oxysulfate:urea ratios are 1:25 (i.e. close to neutral pH) and 1:50 (i.e. strongly basic synthesis media), resulted in extremely lower rutile phase fraction, 2.9% and 1.4% ,respectively. The coated samples' morphology showed that the entire coating was smooth. When compared to samples with lower rutile phase fractions, those with greater rutile phase fractions exhibit higher reflactance in the visible area, according to the optical performance of the samples. The color value measurments have also revealed that, samples with higher rutile fractions exhibit higher lightness values (L) in comparison to those with lower rutile phase fractions. The study showed that, in general, controlling the rutile phase fraction by adjusting the pH of the synthesis media using in-situ urea decomposition was effective in producing TiO_2 coatings with higher rutile phase fractions and better surface smoothness, which in turn results in higher optical quality.*

Keywords: Pearlescent pigment; α-Al_2O_3; Synthesis; TiO_2 Coting; Optical quality

TABLE OF CONTENTS

CONTENTS

DECLARATION OF ORIGINALITY ii

ACKNOWLEDGEMENT iii

ABSTRACT iv

TABLE OF CONTENTS v

LIST OF FIGURES x

LIST OF TABLES xii

LIST OF ACRONYMS xiii

1. INTRODUCTION 1

1.1 Background of the study 1

1.2. Statement of the problem 2

1.3. Objectives 4

1.3.1. General Objective 4

1.3.2. Specific Objectives 4

1.4. Significant of the Study 4

1.5. Scope of the Study 4

1.6. Research questions 5

2. REVIEWS OF RELATED LITERATURE 6

2.1 Color 6

2.2 Pigments Type 7

2.2.1 Organic pigments 7

2.2.2 Inorganic pigments 8

2.2.3 Difference between Organic and inorganic pigments 10

2.3 Optical properties of pigments 10

2.4 Special effect pigments 11

2.4.1 Metal effect pigments 11

2.4.2 Pearlescent pigments 12

2.4.3 How Pearlescent Pigments Work 13

2.5 Pearlescent pigments basic classification 14

2.5.1 Essence of natural pearl 15

2.5.2 Simple lead carbonate 15

2.5.3 Oxygenated bismuth 16

2.5.4 Flakes of titanium dioxide 16

2.6 Substrate-based effect pigments 17

2.6.1 Using mica platelet-based pigments 17

2.6.2 Pigments made from flakes of alumina 18

2.6.3 Pigments made from flakes of silica 19

2.6.4 Pigments based on glass flakes 20
2.7 Structural features of titania polymorphs 20
2.9 Previous efforts to tackle the challenge 23
2.10Alternative method 27
2.10.1 Phase transition hypotheses from the past 27
2.10.2 Phase nucleation depending on solution chemistry 29
2.10.3 Manipulating synthesis parameters in favor of rutile phase formation 30
2.11 Techniques employed in analysis to examine inorganic layers in effect pigments 32
2.12 Research Gap 32
3. MATERIALS AND METHODS 34
3.1 Materials 34
3.2 Chemicals 34
3.3 Methods 35
3.3.1 Alpha alumina synthesis 35
3.3.2 TiO_2 coating 37
3. 4 Design expert with RSM 39
3.5 Particle size measurement: 41
3.6 Rutile phase fraction calculation 41
3.7 Sample characterization 41

3.8 Experimental instruments used on the research work 42
3.8.1 Brunauer–Emmett–Teller (BET) measurement 42
3.8.2 Scanning electron microscopy (SEM) test 42
3.8.3 X-ray diffraction (XRD) test 42
3.8.4 UV/VIS/NIR spectroscopy test 43
3.8.5 Color index measurement 43
3.9 Data collection 44
3.9.1 Secondary data 44
3.10 Method of Data Analysis 44
4. RESULTS AND DISCUSSION 45
4.1 Characteristics of the synthesized α-alumina 45
4.2 Statistical Analysis of the Experimental Results 47
4.3 Results of the coating experiments 49
4.4 Statistical Analysis of the Experimental Results of Color value 56
4.5 Condition optimization and confirmation test 59
4.6 Performance analysis of synthesized pigment 59
4.7 Color characteristics of the samples 60
5. CONCLUSION AND RECOMMENDATION 62
5.1 Conclusion 62

5.2 Recommendation 63

5.2.1Recommendations from this Study 63

5.2.1Recommendations for Further Study 63

REFERENCES 64

APPENDIX 70

LIST OF FIGURES

Figure2.1: Visible light with wavelength difference between spectra colors 6

Figure 2.2: Naturally extracted organic pigment..... 8

Figure 2.3: combination inorganic pigment 9

Figure 2.4: Optical properties of absorption pigments, effect pigments and natural pearls..... 11

Figure2.5: Eco friendly natural pearl 13

Figure 2.6: Simplified diagram showing the optical behavior of pearlescent pigments constituted by substrate and high refractive coating. 14

Figure 2.7: Natural pearl essence 15

Figure 2.8: Arrangement of [TiO_6] in titania polymorphs 21

Figure 2.9: SEM micrographs of (a) P4, (b) P8, (c) P13 and (d) P17 specimens 24

Figure 2:10: SEM micrographs of mica-titania pigments; (a) TiO_2/mica, (b) 0.66% SnO_2/TiO_2/ mica 25

Figure 2.11: SEM micrographs of micaetitanium pigments: (a) micaeTiO_2, (b) mica-2.07%MnO_2-TiO_2. 26

Figure. 2.12: Orientation of third [TiO_6] in linear and zig-zag fashion. 28

Figure 2.13: Several types of OH bridges can be formed by olation condensation process 30

Figure 2.14: Hydrothermal synthesis of TiO_2 31

Figure2.15 Orientation of the third [TiO_6] in linear and zigzag fashion 31

Figure 3.1: Process flow of α- Al_2O_3 with TiO_2 pearlescent pigment..... 35

Figure 3.2: Process flow of α- Al_2O_3 synthesis 36

Figure 3.3: Process fellow of synthesizing process of Alpha alumina 37

Figure 3.4: Process flow TiO_2 coating on α-Al_2O_3 powder 38

Figure 4.1 XRD pattern of the synthesized powder 45

Figure 4.2 SEM images of: (a) synthesized α-Al_2O_3 powder, (b) Commercial Mica powder 46

Figure 4.3: Higher and lower magnification images of as coated α-Al_2O_3 powders 50

Figure 4.4: The XRD patterns of the as coated α-Al_2O_3 powders at different urea concentration 51

Figure 4.5: The XRD patterns of heat-treated TiO_2/α-Al_2O_3 powders at different oxysulfate/urea ratio 52

Figure 4.6: Higher and lower magnification images of heat treated TiO_2/α-Al_2O_3 powders 53

Figure 4.7: portion of the XRD patterns of the heat-treated TiO_2/α-Al_2O_3 where 100% rutile and anatase TiO_2 peaks belong 54

Figure 4.8: Diagnostic plot for the fitted model 57

Figure 4.9: Effect of three parameters (temperature, concentration and time) on alpha alumina/tatania pigment (a) response surface and (b) contour plot of the experiment of Color value 58

Fig 4.10: The spectral reflectance curves of Alumina/titania pigments with different pH conditions: (a) 1.5 (b) 1.25 (c) 1.50 60

Fig 4.11: Color characteristics of the samples 61

LIST OF TABLES

Table2. 1: Rutile and anatase mole percent in mica-titania pigments 25
Table2.2 Color characteristics of the sample 26

Table3. 1: The levels used for concentration, temperature and time 39
Table3. 2: Different parameters to evaluate the Color value (whiteness) 40

Table 4: 1 Surface area and average particle size of synthesized α-Al_2O_3 and commercial mica 46
Table 4: 2 Analysis of variance results for acquired mode 47
Table 4: 3 R-squared (R^2) value for the model 47
Table 4: 4 Statistical summaries for each model 49
Table 4: 5 Rutile phase fraction 55
Table 4: 6 Different paramenter to evalute the color absorbance test 56
Table 4: 7 Lightness results of samples 61

LIST OF ACRONYMS

PVD ……..……Physical vapor deposition

pH ……..…Negative logarithm of concentration of hydrogen ion

HDPE …….High-Density Density Poly Ethylene

SEM ……. …. Scanning electron microscopy

XRD ……. X-ray diffraction analysis

VMP…….. Vacuum Metallized Pigment

TEM…….Transmission electron microscopy

BET ……..….... Brunauer–Emmett–Teller

ART ……..……. Anatase-Rutile transformation

R^2 …….Correlation coefficient

RSM …….Response surface methodology

ANOVA……. Analysis of variance

1. INTRODUCTION

1.1 Background of the study

Numerous industrial goods and end-user applications have Shiny, iridescent, and angle-dependent optical effects are present in a wide range of industrial products and end-user applications. These effects are used in both decorative and practical applications, such as automotive paints, plastics, printed goods, security printing, and optical filters. For example, angle-dependent optical effects are hard to replicate with photocopying or copier technology in the security industry. Since forging is limited to similar goods, it is significantly more expensive and complex. Because of this, many countries use optical and pearlescent multilayer pigments on their banknotes.(Maile et al., 2005).

The use of unique effect pigments has numerous advantages for decorative applications. First, a multitude of platelet-like, semi-transparent particles of a pearlescent pigment are arranged to provide the appearance of optical depth. The final impression is the consequence of light reflection at various pigment-binder interfaces as well as at the effect of the pigment's own boundary layers. Such an effect is especially prominent when extended portions are contoured as in-vehicle fenders (Podszus E., 1923)

The polymorphic TiO_2 is a nanomaterial that has undergone extensive research due to its unique features and significant roles in resolving the environmental and energy crises through efficient solar energy consumption. The groundbreaking study on the use of a TiO_2 electrode in photocatalytic water splitting has spurred research into its potential uses in a variety of fields, including photo catalysis, photovoltaics, batteries, photonic crystals, UV blockers, smart coatings, and fillers for textiles, paints, papers, cosmetics, and biomedical sciences (X. Lang, X. Chen and J. Zhao, 2014).

Titania has a number of exceptional qualities that make it special, including a high redox potential, low cost, non-toxicity, good resistance to harsh environments, hydrophilicity, humidity and gas sensing, dielectric character, advantageous band edge placements, ease of fabrication with a variety of morphologies(Zhang et al., 2018).

Alpha-alumina is a thermodynamically stable phase with a number of characteristics, including high hardness, chemical stability, and thermal stability (melting point is around 2051 °C). α- Al2O3 platelets have attracted important attention due to their combination of the plate- suchlike shape and superior

natural performance, similar to high strength, high modulus, and chemical resistance (Y. Yoshizawa etal., 1998). Indeed, these particular platelets have been used considerably as mounts to design and fabricate metal, polymer or pottery mixes to ameliorate their mechanical parcels including elastic modulus, durability, and strength, since the commerce between platelets and matrix induces energy dispersion or stress transfer (Li- Hui & Qing- Wei, 2011). also, another large-scale operation of the α- Al_2O_3 platelets is serving as a substrate for iridescent color which is veritably useful as a raw material for maquillages, plastics, inks, cosmetics, and glazes. In these operations, the scale of α- Al2O3 platelets, including the consistence and aspect rate (proportion of periphery to consistence), is a crucial factor that influences the performance of products.

This work shows that a regulated demitasse growth process in molten salts can be used to manufacture flakes of alumina (α-Al_2O_3, corundum). Following washing, extremely thin flakes of corundum are formed, exhibiting a high aspect ratio, a limited distribution of consistency, and extremely smooth surfaces. The investigation of a smooth coating surface was carried out by coating alpha alumina with titanium. High rutile phase fraction and high optical quality were investigated by analyzed the sample morphology, Surface area crystalline structure, optical quality, and color index of the sample.

1.2. Statement of the problem

Usually, metal oxide layers are deposited on mica in an aqueous suspension, and then the mica is calcined to make mica-based pearlescent colors. In case of mica-titania pearlescent pigments, precursors like titanium oxysulfate ($TiOSO_4$), titanium oxychloride ($TiOCl_2$) or titanium tetra chloride ($TiCl_4$) undergo hydrolysis in the aqueous media resulting in the deposition of the amorphous titanium hydroxide ($Ti(OH)_4$) on the mica surface. Heat treatment is followed after deposition of the amorphous titania on mica, to obtain the high refractive index crystalline TiO_2 phases. The pearl like luster becomes more apparent if the refractive index difference between the coated metal oxide and the substrate is larger(Gao et al., 2012). The rutile phase has the highest refractive index among all TiO_2 polymorphs thus, is the most preferable phase as a coating layer in TiO_2/mica pearlescent pigment.

However, the majority of methods used to synthesize titania result in the kinetically advantageous polymorph of anatase; from there, as we previously documented, the anatase-directing effect of mica

pigments can be produced by doping and high-temperature calcination (Gao et al., 2012). At 1000˚C, the calcination temperature, however, anatase is still present. (R.Song et al., 2005).

Thermal expansion coefficient mismatch between mica and titania and the associated thermal stress and crack formation is an issue during high-temperature calcination. Formation of cracks in the coating layer results in scattering of light and the consequent decline of pearl luster. Thus, finding means by which low temperature rutile phase transformation can be possible to have paramount importance in obtaining better pearlescent effect.

(Topuz et al., 2011)Previous researchers have attempted to achieve low temperature rutile phase formation following different approaches such as, using rutile directing substrate like alumina, pre-coating the mica with MnO_2 and SnO_2 which have similar crystal structure as rutile TiO_2, and Fe and other metal doping. The attempts have resulted in higher rutile phase fraction on the final coating but in most cases with compromised optical quality.

The attempts were not effective enough to result in smooth coating along with high rutile fraction, which leads to light scattering due to rough surface coating and consequent optical quality degradation. Proper control of the hydrolysis kinetics of TiO_2 precursors is usually the key in obtaining smooth surface deposition. Thus, in this study, important kinetic parameters those are temperature ,time and pH ,which have also impact on low temperature rutile phase formation will be investigated to obtain high rutile fraction along with, better coating smoothness.

1.3. Objectives

1.3.1. General Objective

The main objective of the research was A Study on Optical Quality Enhancement of Alpha-Alumina/Titania Pearlescent Pigment via Insitu pH Control.

1.3.2. Specific Objectives

- To evaluate the synthesis approaches for nano-coating TiO_2 on α-Al_2O_3.
- To determine the optimum operating parameters (temperature, pH, and time) for coating TiO_2.
- To analyze the surface evaluation of the coated α-Al_2O_3 and the degree of crystallization as a function of temperature.
- To assess the optical performances of the developed α-Al_2O_3 based pigments.
- To evaluate and compare the performance of synthesized pigment.

1.4. Significant of the Study

This study will provide information about the Surface coating of α-Al_2O_3 with TiO_2 Nano-particles for special effect (pearlescent) pigment, which enables the company or any other concerned body to think about how better optical quality can be synthesized and for pigment industries those typically lack mechanical stability, making them unsuitable for use in technical applications where stress is applied.it will also provide to pigment industries those use pearlescent pigment, and have optical and mechanical property limitation and Suggest ways by which pigments with better optical quality can be synthesized . The study will benefit the pigment industries and can be the source of information for further study in the area.

1.5. Scope of the Study

The scope of this research work is Synthesis of high aspect ratio, smooth surface alumina flakes by using ($Al(OH)_3$ and Salts), TiO_2 coating using co-precipitation technique with $TiOSO_4$ as TiO_2 precursor, urea as hydrolyzing and pH controlling agent.α-Alumina/Titania pearlescent pigment with large rutile phase fraction and consequent better optical quality, testing overall performance property by using standard device , such as Scanning Electron Microscopy (SEM) to study the morphological effects of pigments;

most of the intriguing aspects can be accessed through this method., X-ray diffraction analysis (XRD) for the crystal structure determination of TiO_2 on α-Al_2O_3 and Optical properties To investigate the optical properties of the pigments by measured Spectrophotometer (D65 illuminant).

1.6. Research questions

1. Does the precursor substrate influence the optical quality of the final alpha alumina/titania pearlescent pigment?
2. Does the operating parameters such as temperature, pH, and time effect on coating TiO_2?
3. Does the coated α-Al_2O_3 have impact on degree of crystallization as a function of temperature difference?
4. Does the nano-coating TiO_2 on α-Al_2O_3 influence on smooth coating and optical quality of the pigment?
5. Does the temperature variation affect the coating process?
6. Does the pH condition affect titanium oxide phase transformation?

2. REVIEWS OF RELATED LITERATURE

2.1 Color

The mortal eye can describe visible light, which is a small part of the electromagnetic diapason that includes radio swells, broilers, infrared radiation, visible light, ultraviolet light, X-rays, and gamma rays. Visible light swells correspond to colorful wavelengths that are perceived as varied colors The color we see is a result of those wavelengths that are reflected to our eyes (Grzybowski & Kupidura-Majewski, 2019)Whether synthetic or natural, all colorings and colors are complex organic composites with a" color- bearing" element called a chromophore, which is frequently a short conjugated system(a chain of tittles joined by interspersing single and double bonds), in their molecular structures.

Pigment and dyes are substances that give a material color. Both dyes (also known as dyestuffs) and pigments are constantly appertained to as colorings. The size of the patches is the primary distinction between pigments and dyes. Pigments are significantly coarser than dyes. When applied to a material, dyes also referred to as colorants which contain dissolved coloring ingredient are absorbed by the material(Chamoli et al., 2021).

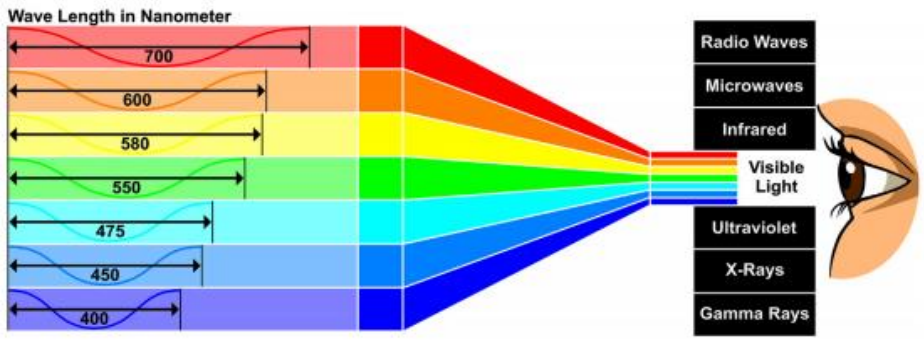

Figure2.1: Visible light with wavelength difference between spectra colors

Source: Grzybowski & Kupidura-Majewski, 2019

Pigments are the composites added to accoutrements to give them color. This deceptively simple operation has shaped our perception of the world via art, fashion, and indeed computer displays and drugs. Pigments are the base of all maquillages, and have been used for glories. They're base multicolored material. Beforehand colors were simply as ground earth or complexion, and were made

into makeup with spit or fat. Ultramodern colors are frequently sophisticated masterpieces of chemical engineering. This exhibition includes most important colors used through the early 20th century(Maile et al., 2005).

Titanium dioxide pigment is fine white greasepaint. When used in maquillages, it provides for maximum sanguineness and nebulosity. It gives makeup high caching power, meaning the capability to mask or hide the substrate underneath. It does this more effectively than any other white color. Titanium dioxide, a chemical patch with the formula TiO_2, is also appertained to as titanium (IV) oxide or titanium. It's also known as titanium white, Pigment White 6(PW6), or CI 77891 when used as a color. In malignancy of the fact that mineral forms can appear black, it's a white solid that's undoable in water. It can be used as a color in numerous different products, similar as makeup, sunscreen, and food coloring.

To give TiO2 the necessary dissipation, photo activity, and nebulosity for a given operation, its face treated with one or further inorganic oxides, similar as alumina, silica, zirconia, or an admixture of these inorganic oxides, and organic motes, similar as polyhydric alcohol. Because titanium dioxide coatings are frequently veritably thin layers, a fairly high volume of TiO2 color must be employed in coating operations to gain the asked caching effect on the coating subtracts(Mazzella, 2007).

2.2 Pigments Type

Pigments can be divided into two groups according to how they are made: inorganic pigments and organic pigments.

2.2.1 Organic pigments

Organic pigment is uprooted from living organisms (plants and animals) and they've been used for centuries. Extraction of the pigments from plants and animals involves leaching**,** concentrating, drying, powdering, and combining into a formulation (V. Stengl et al., 2003). With the exception of painters' maquillages, organic pigments are often less common than inorganic colors. However, because this approach enhances the color quality of a yield, organic colors are consistently utilized in combination with inorganic colors on a smaller scale (Chamoli et al., 2021). From organic color the following are:

- **Alizarin pigment:** Alizarin crimson is a fabricated pigment that became popular in the early 1800s. It is made from the root of the madder plant, which also yields Alizarin dye. This pigment, also referred to as madder red, can be used to create a variety of red and reddish-purple hues.
- **Azo pigments:** are distinguished by the presence of a nitrogen group, but they are notable in history for being among the earliest synthetic organic pigments. Azo pigments are the source of many organic red, orange, and yellow pigments available on the market today. They are also noticeably more colorfast than many other forms of organic pigments..

Figure 2.2: Naturally extracted organic pigment

Source: Results in Chemistry 5 (2023) 100733

2.2.2 Inorganic pigments

Our environment is dramatically altered by inorganic pigments. They are necessary for coloring structures since they are used in everything from concrete to artist's maquillages, fake maquillages to photocopier color, food coloring to catalytic raw materials. accessories. These colors may be manufactured or derived from minerals. Produced through truly easy chemical procedures like oxidation(Chamoli et al., 2021).

One significant order of inorganic colors are mixed substance oxide colors, sometimes appertained to as complex inorganic color colors. They stand for the colors that are blue, green, pusillanimous, brown, and black. Because of the presence of two or further distinct substance in their composition, these colors are known as mixed complexes. Their main advantages are high ambiguity, heat stability, useful infrared

parcels, light- and downfall fastness, and chemical resistance (Chamoli et al., 2021). They are modeled on several demitasse clear structures, including those of hematite, proud ritual, mock brookite, rutile, spinel, and inverse spinel.

A common inorganic pigment with good color quality, strong hiding power, and affordable price is titanium dioxide. Iron Blue, containing iron, was initially used in cloth dyes. White extender clays are used for this purpose. Metallic pigments, created using metals like bronze and aluminum, give black inks. Blank pigments impart black color, while cadmium pigments provide yellow, orange, and red colors for various materials. Chromium oxide is used in painting for green, yellow, and orange colors (Chamoli et al., 2021).

(Chamoli et al., 2021)Metal oxide pigments are more stable than metal salt pigments. They are less reactive and less soluble in water. Metal oxide pigments are often used in the production of ceramics, glass, and other materials that require high-temperature processing. Metal salts and metal oxides are two different types of compounds that are used in the production of pigments. They are also more reactive and can be used to produce a wider range of colors. Metal salt pigments are often used in the production of paints, dyes, and inks (Chamoli et al., 2021).figure2.3 shows different combination of inorganic pigment.

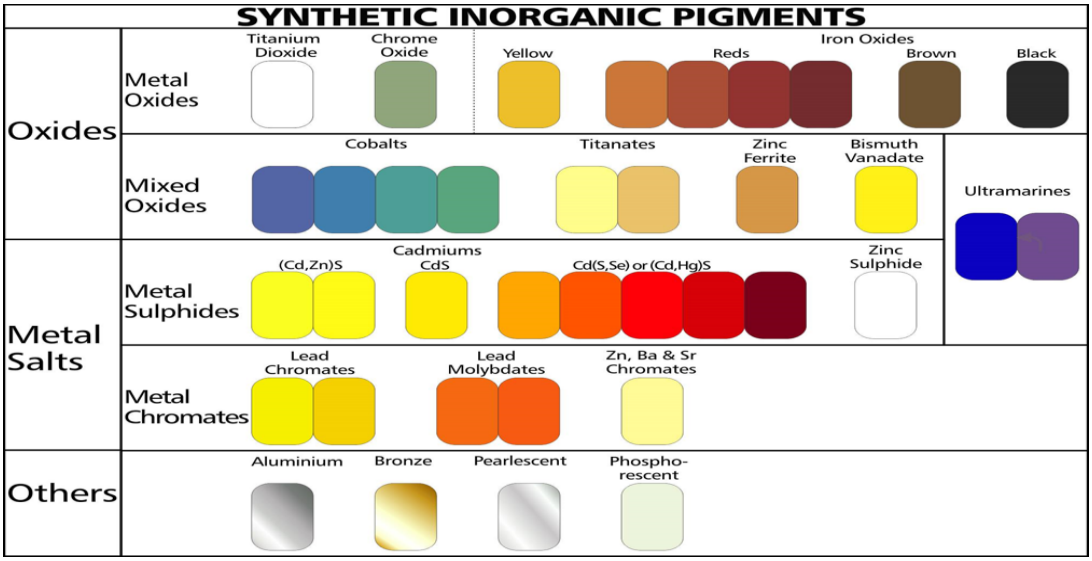

Figure 2.3: combination inorganic pigment

Source: https://vibron.com.au/inorganic-pigments-for-plastics/

2.2.3 Difference between Organic and inorganic pigments

(Chamoli et al., 2021) Although there are fundamental chemical differences between organic and inorganic pigments, there are other distinctions as well. Think about the following distinctions between organic and inorganic pigments when contrasting the two types of pigments:

Although organic pigments have a shorter shelf life, they are typically brighter and have superior tonal quality. Inorganic pigments are more reliable due to their better color retention in light and heat. They offer a wider range of colors and are more economical than organic pigments due to minimal manufacturing processes. Large-scale manufacture can more easily employ and distribute inorganic pigments. Whereas organic pigments absorb light through conjugated double bonds, they absorb light by electron transfer. Organic pigments have a greater surface area and produce bolder, brighter colors than inorganic pigments, which are transparent due to their bigger particle sizes(Chamoli et al., 2021).

2.3 Optical properties of pigments

Natural or artificial special effect pigments provide exceptional levels of shine, brilliance, and opalescent color products that are based on optically thin layers (Mirhabibi, 2014). The development of this visual print is caused by light dispersion and reflection on thin multiple layers. The vibrant optical principles of metal effect pigments (B), pearls (C) and pearl luster pigments (D), and typical pigment pigments (A) (absorption pigments) are shown in Figure 2.4.The most significant category of pigments with distinctive effects. When it comes to absorption pigments, diffuse scattering and/or absorption are the basis for light interaction.

The metal effect pigments and pearl luster effect pigments belong to a group of effect pigments that exhibit entirely different optical characteristics.(Mirhabibi, 2014) Small metal platelets, such as those made of copper, titanium, or aluminum, make up metal effect pigments. These platelets function like tiny glasses, reflecting almost the entire incident light.

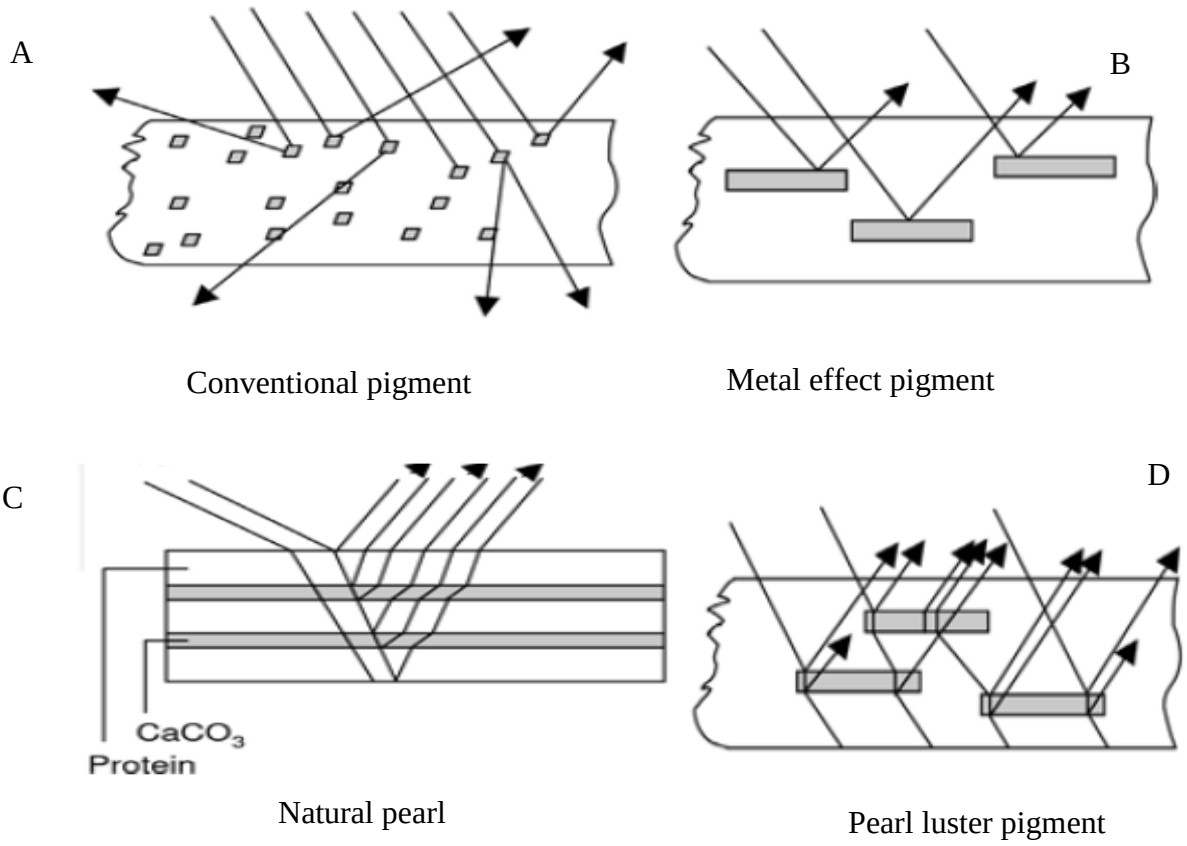

Figure 2.4: Optical properties of absorption pigments, effect pigments and natural pearls

Source: https://www.researchgate.net/publication/221925909-Ceramic-Coatings-for-Pigments

2.4 Special effect pigments

Because special effect pigments enable the carrying of odd optical goods, diligence is becoming more and more interested in them. can be used in a variety of processes, including those in the plastics, automotive, and cosmetics industries (L.M. Greenstein, 1998). The metallic flake, pearlescent, and special effect pigments the three main orders of product colors as well as the diligence that results from these custom coatings. Pearlescent pigments, metal effect pigments, and essence effect colors make up the two main categories of effect pigments.

2.4.1 Metal effect pigments

(Maile et al., 2005) Essence grains are treated using stamping equipment to create metal effect hues. The essence flakes are mostly produced by ball manufacturers utilizing dry milling (Hametag process), wet

milling (Hall process), or both. A lubricant is added to the ball milling process to aid in the cold emulsion and produce the desired leafing or non-leafing parcels. "Cornflakes" and "gray bone" varieties of standard aluminum colors are produced based on the form and quality of the beginning grains as well as the milling parameters(Suyati et al., 2019)

PVD aluminum, sometimes referred to as VMP (Vacuum Metallized Pigment), is a unique kind made using a vacuum process in which aluminum is deposited on a web. When the deposited aluminum is released from the web, extremely thin flakes that resemble sophisticated glass-like products are obtained. These flakes can then be integrated into coating systems.(Li-Hui & Qing-Wei, 2011).

When compared to stretch films, effect pigments provide a number of advantages in both ornamental and utilitarian applications. This product offers simple incorporation into various application systems, blending pigments for diverse color effects, and achieving vivid, textural effects due to single particles. It's easy to manufacture, cost-effective, and environmentally friendly, with flexible application procedures like spraying, printing, and extruding (Maile et al., 2005).

In contrast, extended films are typically only suitable for highly restricted uses or are nearly impossible to utilize at all. As a result, platelet-shaped effect pigment particles are the clear focus of new material development for both decorative and functional effects (such as electrical conductivity and infrared reflection)(Maile et al., 2005).

2.4.2 Pearlescent pigments

A **pearl** is a hard, glistening object produced within the soft tissue (specifically the mantle) of a living shelled mollusk or another animal, such as fossil conulariids. Just like the shell of a mollusk, a pearl is composed of calcium carbonate (mainly aragonite or a mixture of aragonite and calcite) in minute crystalline form, which has deposited in concentric layers (Gemdat G., 2017).

- Pearl Pigments can be broken down it two categories:
    - Natural Substrates: Mica, Kaolin, or Phlogopite
    - Synthetic Substrates: Alumina, Silica, Borosilicate or Synthetic Mica

Figure2.5: Eco friendly natural pearl

Source: *M. Suzuki et al. / Journal of Crystal Growth 433 (2016) 148–152*

(Islam et al., 2015) Natural or artificial pearlescent pigments exhibit remarkable shine, brilliance, and iridescent color effects brought on by light interference or repeated reflections. In order to create these pigments, high refractive index materials like metal oxides are coated over low refractive index materials like mica and silica. Metal oxides such as TiO_2, Fe_2O_3, Cr_2O_3, SnO_2, ZnO, ZrO_2, or complexes of these oxides are frequently utilized for coating. Typically, this coating procedure uses a Sol-gel method, in which the precipitation is accomplished using salt solutions.

Pearlescent pigments can be used decoratively or practically. Cosmetics, plastics, printed products, porcelain, industrial coatings, optical filters, and car paints.(Štengl et al., 2003) Some have further been employed because of characteristics including electrical conductivity, magnetic qualities, and IR reflection(Bayat et al., 2008). The most well-known instances are mica-titania pigments, which are made of TiO2 that has precipitated onto mica platelets.

2.4.3 How Pearlescent Pigments Work

At least three layers of materials with various refractive indices make up pearlescent pigments. Consequently, the pearlescent effect is created by the light beam's specular reflection from the numerous contacts that are present through the pigment's thickness. These pigments' colors are created by the interference of light rays that reflect from the top and bottom surfaces of the metal-oxide layer at specular angles. The hues of these coatings can be gold, red, blue, or green, depending on their thickness. The

pearlescent pigment's operating principle is depicted in Figure 2.3. Because of the great degree of transparency of the mica platelets, white light can travel through them. Reflected travel through oxides of metals. The titanium dioxide layer, derived from metal oxides, has a greater refraction index than the surrounding mica. The ideal distribution of 10 to 60 microns is what gives pearlescent pigments their greatest appearance when light is refracted and reflected at interfaces at varied angles (Maile et al., 2005).

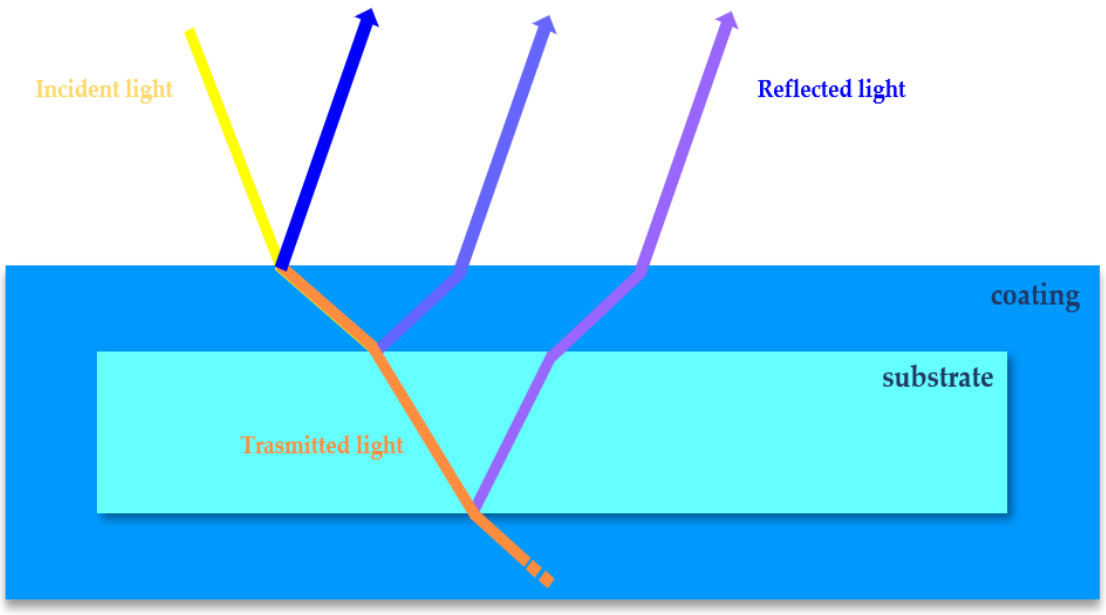

Figure 2.6: Simplified diagram showing the optical behavior of pearlescent pigments constituted by Substrate and high refractive coating.

Source: *https://www.naturalpigments.com/artist-materials/pearlescent-pigments-how-they-work*.

2.5 Pearlescent pigments basic classification

Substrate-free pigments are well-known metal effect pigments, such copper-zinc platelets or aluminum, lack a layer structure. This group also includes transparent effect pigments such as flaky polycrystalline TiO_2 or single-crystalline BiOCl. Most of these non-metallic flakes are extremely thin in order to produce a particular interference color. When compared to flakes based on a substrate platelet, this may result in a reduced mechanical stability (Maile et al., 2005).

2.5.1 Essence of natural pearl

(Shindy, 2016) Fish scales, skin, or bladder are the sources of natural pearl essence, sometimes known as natural fish silver. In order to dissolve and remove the proteins, fish scales are extracted as an aqueous suspension using organic solvents. Scale and purine crystals can be separated from each other in the residual dispersion by an intricate phase-transfer and washing procedure. Since the pigment platelets have a propensity to aggregate, they should only be treated as dispersions. Due to their extremely high cost, these dispersions are almost solely employed in cosmetic applications (nail polishes, lotions, and shampoos) (V. Stengl et al., 2003).

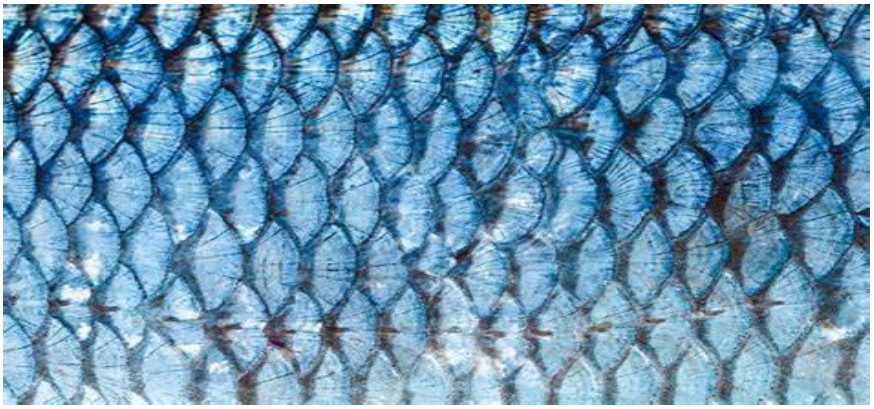

Figure 2.7: Natural pearl essence

Source: *http://sirs.agrocampus-ouest.fr/discardless_wp6/images/composition/FI-19.png*

2.5.2 Simple lead carbonate

Thin hexagonal platelets of basic lead carbonate ($Pb(OH)_2 \cdot 2PbCO_3$) can be produced by precipitating lead acetate solutions in water. These solutions are reacting with carbon dioxide in a much regulated environment. The resulting platelet-shaped particles have diameters of approximately 20 m and a thickness of less than 0.05 m, resulting in an aspect ratio of roughly 200. The platelets have an intense shine because to their uniform surface and high refractive index of 2.0. Pigments with interference hues can be produced by increasing the particle thickness through altered reaction conditions.

Due to their high density of 6.4 g/cm3, which causes them to settle quickly in suspensions, the crystals are extremely brittle. Because basic lead carbonate tends to clump together, it is treated as a stabilized

dispersion. Because of the toxicological hazards, the pigment's use is becoming increasingly restricted. (L. Sung, et al., 2000).

2.5.3 Oxygenated bismuth

Hydrolysis of extremely acidic bismuth salt solutions in the presence of chloride results in the production of bismuth oxychloride (BiOCl) effect pigments. The selected reaction parameters, such as the concentration of bismuth salt, temperature, pH value, reactor geometry, and addition of surfactants, can be used to modify the crystal quality. It is possible to flatten the typically tetragonal bipyramid crystal shape into platelets with a large aspect ratio. Aspect ratio of 10–15 pigments are employed as fillers in cosmetics because they have a low sheen and excellent skin feel. (Ge M et al., 2011).

Higher aspect ratio crystals have a bright sheen and are usually used in nail polish. Technical uses of bismuth oxychloride are limited due to its low light stability, quick settling tendency caused by a density of 7.73 g/cm^3, and lack of mechanical stability. Therefore, it is mainly utilized in jewelry and buttons in addition to cosmetics. (Podszus E., 1923).

2.5.4 Flakes of titanium dioxide

Continuous TiO_2 films can be broken down to create titanium dioxide flakes. These films can be produced by thermally hydrolyzing $TiOCl_2$ on the web's surface during the web-coating process. TiO_2-mica pigments can also provide substrate-free TiO_2 flakes by dissolving the substrate in strong acids or hydroxides (L. Sung, et al., 2000).The titanium dioxide flakes that were obtained in this way are polycrystalline and rather porous rather than single crystals. They can't be utilized in technical applications where stress is applied because they often only exhibit minimal mechanical stability.

TiO_2 is a polymorphous substance that can crystallize as rutile, anatase, or brookite. These polymorphs all share the same underlying octahedral units in a variety of configurations. Rutile TiO_2 is the most stable phase compared to the other two phases, even under extremely acidic or basic circumstances. (Ge M et al., 2011).

Because rutile has a higher refractive index than anatase (2.93), full rutile layers can be used to create mica-titania pigments with vibrant color and sheen. (R.Song et al., 2005). Furthermore, rutile has been found to show poor photocatalytic activities in most cases(Du et al., 2008), which could aid in resolving

the issue that has plagued the coatings industry: "chalking" (photo-oxidation of surrounding polymeric binders in outdoor weathering triggered by the pigment). The rutile modification of titanium dioxide in a pearlescent pigment is preferred over the anatase modification for the reasons mentioned above.

It is widely accepted that the synthesis of phase-pure rutile form at low temperatures is extremely challenging because the majority of methods used to synthesis titania result in the kinetically advantageous polymorph of anatase. Because most of the methods used to synthesise titania result in the kinetically advantageous polymorph of anatase, it is widely thought that producing phase-pure rutile form at low temperatures is extremely difficult (Prorokova et al., 2020). Furthermore, anatase persists up to 1000 °C during calcination because of the mica's anatase-directing function (R. Song et al., 2005). It is possible to achieve rutile alteration of mica-titania pigments by high-temperature calcination and doping.

2.6 Substrate-based effect pigments

(Maile et al., 2005) Platelet-like effect pigments that are not substrate-based can occasionally be brittle and frequently lack mechanical stability. Furthermore, their chemical makeup places limitations on them. As a result, effect pigments based on a substrate serving as a thin optical layer's mechanical support were created. In addition, the substrate serves as a template for the thin layer's creation.

Compared to the non-substrate-based effect pigment, a far wider range of materials can be selected for this layer. The substrate will begin to function as an optical layer and join an optical three-layer or multilayer system if its thickness distribution narrows. Two in-depth reviews of special effect pigments based on metal flakes, silica, alumina, and mica were published in 1999 and 2003.

Titania (both rutile and anatase), iron (III) oxide, mixed titanium–iron oxides, silica (as a low-rea refract layer in multilayer systems), and chromium (III) oxide make up the most significant optical layers.

2.6.1 Using mica platelet-based pigments

(Štengl et al., 2003) 1942 saw the first description of effect pigments based on mica. Due to increased manufacturing repeatability, their commercial popularity began in the 1970s and picked up speed in the mid-1980s with the development of weather-resistant varieties for outdoor use. The most recent noteworthy advancement was the creation of optical multilayer systems on mica towards the close of 1990, in contrast to artificial substrates; naturally occurring muscovite mica is quite cheap and abundant

in the natural world. Its layered silicate crystal structure allows it to split into thinner flakes with a mean thickness of about 200–500 nm. The majority of the mica flakes have sizes between 5 and 200 m (L.M. Greenstein, 1998).

(L.M. Greenstein, 1998) Because of the benefits of metal oxide-mica pigments, over 90% of the global market for transparent effect pigments is made up of this particular group. When compared to natural muscovite, synthetic fluor phlogopite mica has a lower iron concentration and a somewhat whiter bulk tone. This advantage is fairly minor, though, and it hasn't yet resulted in any notable commercial success. Because they only have one optical layer, single-layer mica-based pigments exhibit an interference color that "turns on and off" in relation to natural proportions. Its layered silicate crystal structure allows it to split into thinner flakes with a mean thickness of about 200–500 nm. The majority of the mica flakes have sizes between 5 and 200 m.

A few degrees of color shift are visible when examining the angle dependence of the interference color in detail. Mica effect pigments are usually made by calcining the mica after metal oxide layers have been deposited on it in an aqueous suspension. $TiOSO_4$ (homogeneous hydrolysis) or $TiOCl_2$ (titration) are the starting points for the production of titanium dioxide-mica pigments. TiO_2 can be directly produced on mica as anatase or directly on mica as rutile by employing an intermediary SnO_2 layer.

If the optical thicknesses of the layers in mica-based pigments with many layers are carefully selected, the pigments can exhibit a noticeable angle-angle-dependent effect. But compared to the subsequently described silica flake-basements (e.g., twice the TiO_2-SiO_2-TiO_2 stack plus the optically inactive mica thickness), the mica-multilayer pigments are much thicker and heavier, requiring a higher pigment load for a given color strength (L.M. Greenstein, 1998).

2.6.2 Pigments made from flakes of alumina

Alumina can exist in a variety of states. Alpha and Gama-alumina phases are two of the most significant phases. After being heated to 1000 °C, bohemite forms the alpha phase. It is a thermodynamically stable phase with a number of characteristics, including high hardness, chemical stability, and thermal stability (melting point is around 2051 °C). As a result, it can be utilized to create ceramics, shields, and protective coatings (Mohammed et al., 2020). Gama-alumina phase, on the other hand, is an unstable phase that transforms into phase q when heated to a temperature between 600 and 700 °C. Although it is

employed as a medium in chemical reactions, it cannot be used at high temperatures since it transforms into the phase above 950 °C.

(Mohammed et al., 2020)There are various ways to make aluminum nanoparticles; the Sol-Gel process is one of the most crucial. In comparison to other methods of preparation including ball milling, sputtering, friction stir, laser ablation, and hydrothermal, this method is crucial for creating Nano powders since it is very straightforward, cheap, and requires no complicated equipment. One of the well-known synthetic techniques for producing metal oxide and mixed oxide of substances is called sol-gel .The structural and surface properties of the materials may be controlled using this technology.

The hydrolysis, condensation, and drying processes are basically what the Sol-gel approach entails to get the final metal oxide. Metal oxide is created through a number of subsequent stages. The precursor mineral precursors first go through quick hydrolysis to create a metal hydroxide solution, then instantly condense to create 3D gels. The resulting gel then goes through a drying process. According on the type of solvent employed, the Sol-gel process can be divided into two categories: aqueous and non-aqueous(Horn et al., 1972).

A regulated crystal formation technique in molten sodium sulfate can yield alumina (α-Al_2O_3, corundum) flakes with acceptable optical quality. Following washing, exceptionally thin corundum flakes with a high aspect ratio, a limited thickness distribution, and extremely smooth surfaces are discovered. Special reaction conditions and doping can be used to control the thickness (Pfaff et al., 1998).

When covered with iron (III) oxide or titanium metal oxide, the flakes show a clear directed reflection that is frequently referred to as crystal luster. This can be attributed to the even surface, the relatively uniform particle thickness, and the modified thickness of the metal oxide layer. As a result, the colors based on this substrate frequently have a distinct textural appearance from the other pigments, resembling glitter.

2.6.3 Pigments made from flakes of silica

A specifically created web-coating procedure can be used to produce thin silica flakes (SiO_2) with a very consistent and controllable thickness. The flakes can also be utilized as effect pigment substrate particles to improve color travel and chromatic strength and purity. (M. Levlin, et al., (2001).

2.6.4 Pigments based on glass flakes

The glass flake substrates are comparable to silica flakes in that they are more transparent than alumina and mica flakes. Glass flakes covered with metal oxide have been used as pearlescent pigments since 1963. Nevertheless, the glass flake substrates that have been made accessible have typically been 10 m thick, which makes it impractical to apply these pigments in layers like printer inks and car paints. Recent developments in tin glass fabrication technology have led to the introduction of effect pigments based on thinner glass flakes onto the market. They differ from the latter in having a significantly wider variation of thickness. Therefore, utilizing single-layering on glass flakes does not provide color travel effects. Commercially accessible silver metal-coated glass flakes come in a wide range and very rough (Pfaff et al., 1998).

2.7 Structural features of titania polymorphs

Anatase (a=b=3.785, C=9.514, space group D4h, I41/amd), rutile (a=b=4.593, C=2.959, space group D4h, P42/mnm), brookite (a=b=5.456, C=9.182, space group D2h, pbca), and TiO_2 (B) (a=12) are among the crystalline forms of TiO_2.An octahedron with oxygen ions at its vertices and titanium atoms in the center represents each phase's local order; different spatial figurations share its corners and edges in different ways(Özer, 1992).

It has been demonstrated by theoretical and experimental research that rutile and anatase share a structural relationship. The most thermodynamically stable substance is rutile at all pressures and temperatures; metastable anatase and brookite are kinetic byproducts. Ten additional octahedra, two of which are edge-shared and eight of which are corner-shared, encircle each octahedron in the rutile.

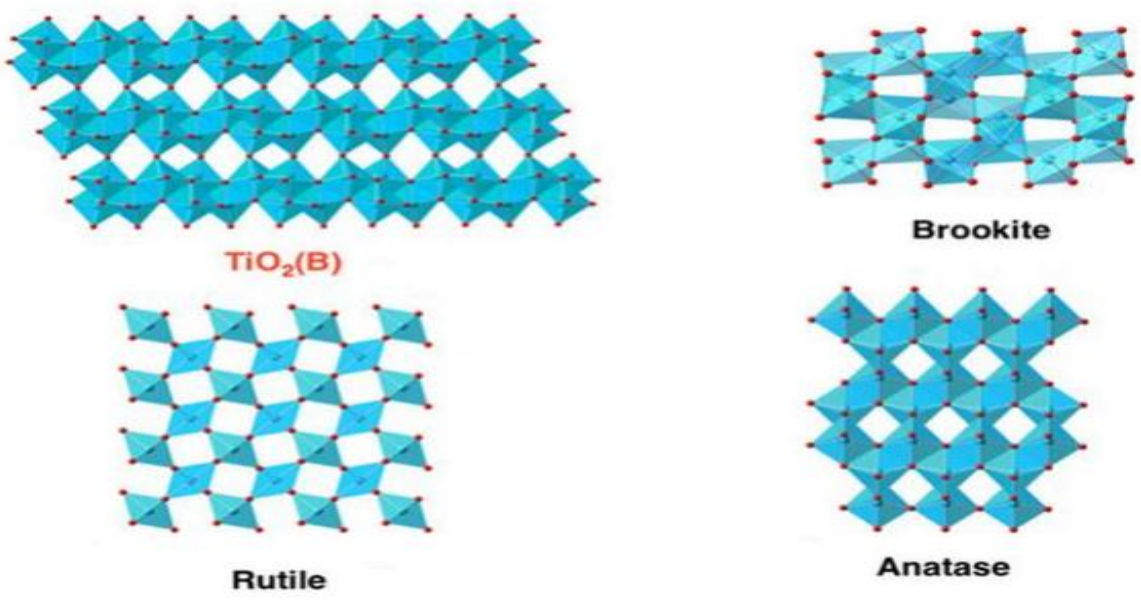

Figure 2.8: Arrangement of [TiO_6] in titania polymorphs

Source: *Chem. Mater. 2007, 19, 2512-2518*

(Ibrahim & Sreekantan, 2011) Eight octahedra (four edges shared and four corners shared) encircle the [TiO_6] in anatase.As a result, a higher fraction of edge-sharing octahedra (50 % vs. 20 %, respectively) is needed to make anatase than rutile. While corner-sharing octahedra require hydrolysis and condensation reaction in the co-ordination sphere, edge-sharing octahedra require the two juxtaposed hydrolysis and condensation process between two octahedra to form. In the primitive tetragonal rutile lattice, the octahedra share two edges to form linear chains parallel to [001], while corner connections along [110] and [110] join the chains. The brookite has an orthorhombic structure with 60 tunnels along the c-axis and octahedra sharing three edges, one of which determines the crystal distribution along the [100] direction and the other two along the [001] direction (R. L. Penn and J. F. Banfield, 1998)

(R. L. Penn and J. F. Banfield, 1999) The low density monoclinic TiO_2 (B) exhibits a somewhat open structure, perovskite-like windows between sites, and edge-and corner-shared [TiO6]. Whereas the unit cell volumes of anatase, rutile, and brookite are 34.02, 31.12, and 32.20 (Å) 3 correspondingly, TiO_2(B) has a unit cell volume of 35.27 (Å) 3.43, 72.In comparison to other titania polymorphs, rutile is clearly more symmetrical and compact.2.8 Hydrolysis of titania polymorphs Rutile crystallized at a pH of 0.5, whereas brookite also formed at this pH range along with rutile. Pure rutile eventually formed in a pH

range of 3.5 to 4.0.369 at pH levels greater than 4, brookite and anatase form crystals instead of rutile. (Ibrahim & Sreekantan, 2011)Therefore, phase change with rising pH (1–7) proceeded as follows: rutile brookite, rutile anatase, rutile brookite, and rutile anatase pH ~0.5 1 - 3 5 - 6 > 6 - 7 Ti(III) is preferentially oxidized during thermolysis as opposed to being hydroxylated, creating acidic Ti(IV) complexes.

Rutile is produced at a somewhat modest rate by the formation of zero charged compounds $[Ti(OH)_4(H2O)_2]^0$ under these acidic circumstances. Along with the correct Ti ratio, brookite is formed either as a result of mixed complexes Ti (III)/Ti (IV) or as a result of partial oxidation of Ti (III). The initial solid oxidation of amorphous TiO_2 occurs at pH values greater than 4.5, and following further heating, anatase crystallizes (Hyoung & Zuo, 2004).

Both phosphates and sulfates have a tetrahedral geometry, with negative ends at the oxygen atoms. They coordinate in a mono, di, and tridentate mode to [TiO6] through a well-known chelate action. The entire octahedron is filled with these ions due to their bonding, which stops rutile formation and chain expansion along the opposing sides. Titania polymorphs are created when trans and cis isomers of the fundamental unit $[Ti(OH)2(H2O)4]^{2+}$ coexist and grow into bigger units. The formation mechanism does not include the participation of oligomer growth units with titanyl Ti=O bond since there is currently insufficient data to support the deprotonation of $[Ti(OH)(H_2O)]_3+$ to yield $[Ti(O)(H_2O)]^{2+}$ (J. Livage, M. Henry and C. Sanchez, , 1988).

(R. L. Penn and J. F. Banfield, 1998) Grain expansion in nano crystallites is understood as the atomic diffusion-driven displacement of grain borders during the coalescence of smaller adjacent grains. When it comes to changing the particle size distribution within the liquid media, nucleation and growth may face competition from processes including aggregation and coarsening.

The phase transition rate and particle growth dynamics are the key mechanisms that regulate the final particle size, shape, and phase composition. The aqueous conditions syntheses are classified using the two regimes of synthesis at low and high temperatures. Once formed, TiO_2 particles are unstable and precipitate to form large aggregates. These aggregates then collapse to form very small aggregates during peptization. It is believed that using this method to obtain the crystalline phases at a low temperature works well. (J. L. Look and C. F. Zukoski, 1992).

2.9 Previous efforts to tackle the challenge

Two approaches have been followed to effect low temperature anatase to rutile phase transformation of TiO_2 coating and using Rutile directing materials.

- **SiO_2, AlN, and TiO_2 coated mica-based pigments**

Created mica-titania pigments by hydrolyzing titanium tetrachloride above mica flakes without calcining them, and they looked at how MnO_2 affected the anatase-to-rutile transition (Saini, p., et al., 2012). Aluminum nitride (AlN) and silica (SiO_2) nanoparticles were frequently utilized as nano fillers in polymer composites (Qin, 2018). Because to SiO_2's great specific surface area, low density, strong thermal and chemical stability, and high The surface and cross-section SEM image as show uncoated mica and SiO_2, AlN, and TiO_2 coated mica-based pigments are given in Figure at different magnification. As seen in the figure many small broken parts observed on the surface and cross-section of uncoated mica. The surface and cross-section SEM image of uncoated mica and SiO_2, AlN, and TiO_2 coated mica-based pigments are given at different magnification(Topuz et al., 2011).

The UV-vis absorption between 350 and 200 nm wavelengths was observed in the optical characteristics of uncoated mica, mica@SiO_2, and mica@AlN pigments. Uncoated mica exhibited a higher absorption intensity. When compared to uncoated mica, mica@SiO_2, and mica@AlN pigments, the absorption value of mica@TiO_2 pigment was wider and greater in the visible range. The mica@TiO_2 pigment was observed to exhibit high optical absorption at wavelengths less than 400 nm. Mica-based pearlescent pigments covered with SiO_2, AlN, and TiO_2 were created in order to determine their thermal, optical, and dielectric properties. The morphology of the pigment demonstrated that SiO_2 and AlN were constantly being deposited on mica flakes. However, the TiO_2 particles were scattered and slightly clumped together on the mica surface. Thermal stability was lowest and UV-vis absorption values were highest when TiO_2 was doped on the mica surface. The significant EM wave absorption performance was not demonstrated by the mica@SiO_2 and mica@AlN pigments.

- **Optimization of the synthesis of a nano-sized mica-hematite pearlescent pigment**

(Tohidifar et al., 2008) Based on the usual hydrolysis process, mica (muscovite), urea, and iron sulfate (III) were regarded as coating precursor, precipitant, and substrate, respectively, for mica-hematite pearlescent pigment. SEM micrographs of the P2 and P10 samples, in that order. (Tohidifar et al. 2008)

It is discovered that the P2 specimen's fast reaction time and low urea concentration prevented some of the mica's surface from being fully coated. Due of the low temperature, the P10 specimen yielded the same result.(Ibrahim & Sreekantan, 2011). Fig.2.9 (b) displays the P8 specimen's SEM micrograph. Additionally, it is evident that the excess urea causes the hematite particles to settle on mica as agglomerated precipitates.

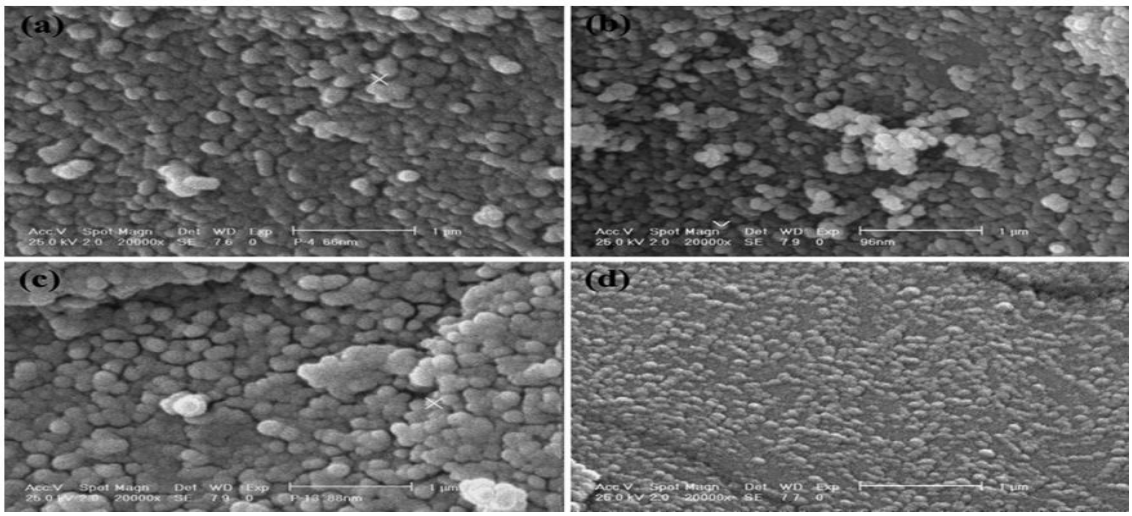

Figure 2.9: SEM micrographs of (a) P4, (b) P8, (c) P13 and (d) P17 specimens

Source: Materials Chemistry and Physics 109 (2008) 137–142

- **Pre-coating mica with Rutile directing materials**

Pre-coating mica with Rutile directing materials due to their crystal structure similarity like

(a) SnO_2 and (b) MnO_2 Coting are reported 95% rutile phase is achieved in case of (a) but the coating smoothness becomes worse (Topuz et al., 2011)

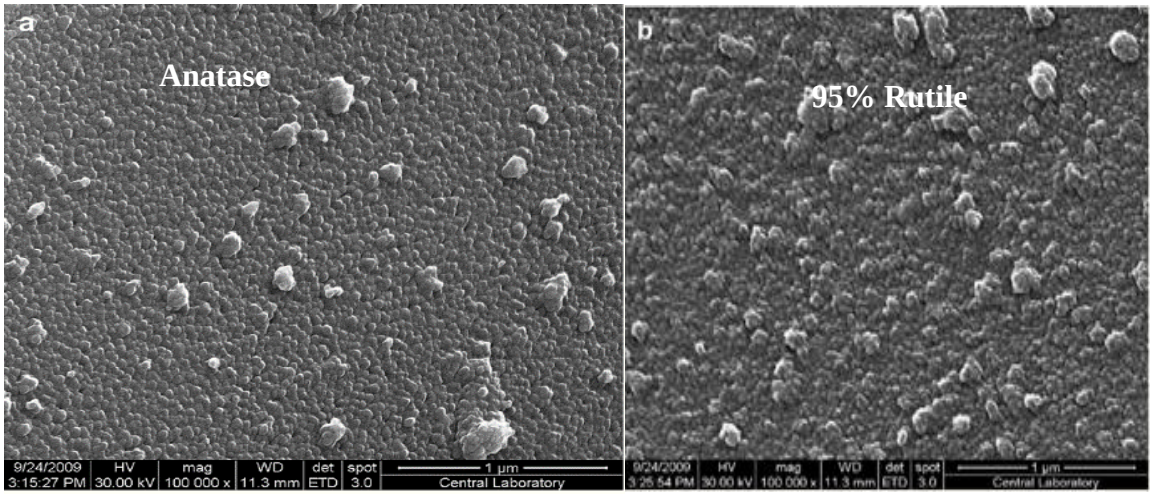

Figure 2:10: SEM micrographs of mica-titania pigments; (a) TiO_2/mica, (b) 0.66% SnO_2/TiO_2/ mica.
Source: Dyes and Pigments 90 (2011) 123-128

Table2. 1: Rutile and anatase mole percent in mica-titania pigments

Sample	Rutile (Mole %)	Anatase (Mole %)
Mica-titania	2.55	97.45
Mica-titania (0.22% SnO_2)	24.55	75.45
Mica-titania (0.44% SnO2)	71.28	28.72
Mica-titania (0.66% SnO2)	95.64	4.36
Mica-titania (0.88% SnO2)	91.64	8.36

Source: *Topuz et al. / Dyes and Pigments 90 (2011) 123-128*

(b) Rutile TiO_2 coated micaetitania pigments were synthesized by hydrolysis of titanium tetrachloride and the effect of MnO_2 on the anataseerutile transformation. They achieved 100% rutile phase but optical quality is compromised due to high rough nature of the rutile coating.

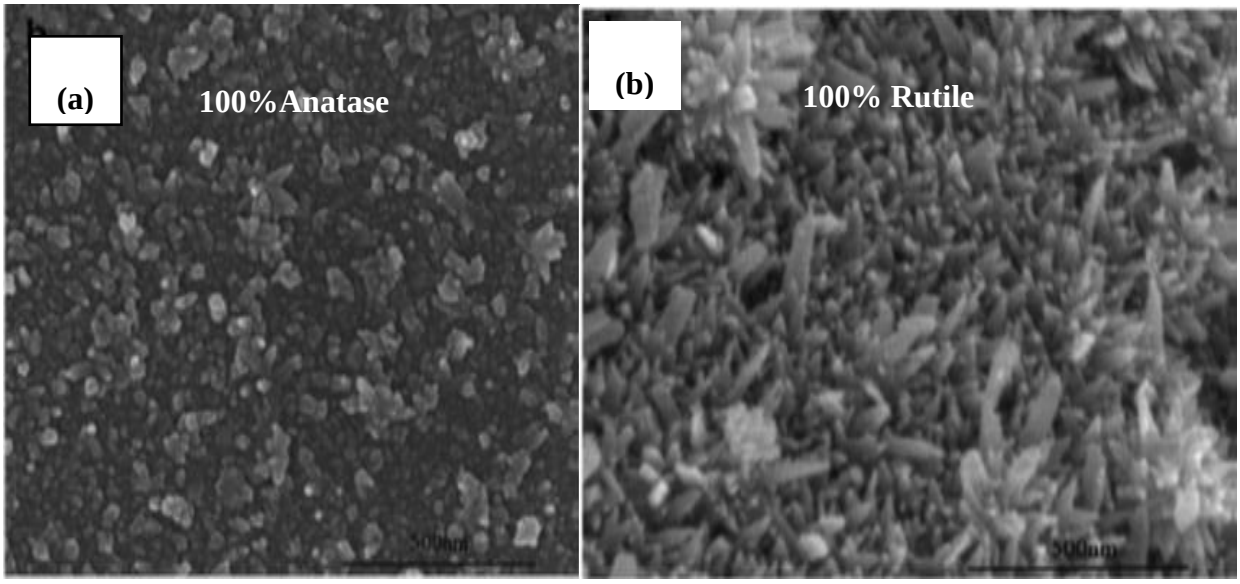

Figure 2.11: SEM micrographs of micaetitanium pigments: (a) micaeTiO_2, (b) mica-2.07%MnO_2-TiO_2.

Source: *Dyes and Pigments 95 (2012) 534-539*

Table2.2 Color characteristics of the sample

Sample	Color coordinates			
	L*	a*	b*	
MicaeTiO_2	90.07	0.15	1.99	1.99
Mica 0.69%MnO_2-TiO_2	89.97	3.20	9.30	9.84
Mica-1.38%MnO_2-TiO_2	84.09	6.24	16.17	17.33
Mica-2.07%MnO_2-TiO_2	83.14	7.58	19.15	20.59

L*, lightness; a*, red-green index; b*, yellow-blue index; C*, Chroma

Source: *Q. Gao et al. / Dyes and Pigments 95 (2012) 534e539*

- **Utilizing the rutile directing substrate (α-aumina)**

Alumina is one of the most commonly used ceramics. This is due to its unique properties, such as high hardness, good thermal and chemical stability, high strength, high young modulus and low price.

Mica is a mineral extracted from earth's crust thus consists of different cations (Si^{4+}, Al^{3+},Mg^{2+}, k^{+}) than alumina (Al^{3+}) which can diffuse in to TiO_2 structure and interfere in the anatse to rutile phase transformation process(Byrne et al., 2019).

2.10Alternative method

2.10.1 Phase transition hypotheses from the past

Fundamental kinetic and thermodynamic problems are involved in the transformation of the titania polymorphs. The linearity of the rutile arrangement allows the Ti-Ti bond to relax, which is thermodynamically advantageous. However, statistical evidence suggests that anatase/brookite nucleation is more likely to occur when the arrangement is at a right angle. Anatase-type crystallites appear to form during the crystallization process before rutile-like crystals, but as rutile crystallizes, anatase nucleation is either suppressed or changes into rutile (Y. Li, T. J. White and S. H. Lim, J, 2004).

Phase transitions are generally characterized as rutile-anatase-brookite-rutile. In the event that the system already contains rutile nucleus, anatase or brookite converts straight into rutile. The second process involves the interconversion of anatase and brookite nuclei, resulting in the conversion of anatase-brookite to rutile (Y. Hu, et al., 2003).

When hydrothermal treatment is applied to an aqueous solution, the most stable phase re-precipitates, causing one phase to dissolve through surface protonation (as in ART) or hydroxylation (as in ABT or BAT). This process is known as the dissolution precipitation pathway. Solid-state interface nucleation is how the ART works during air-based calcination. In this mechanism, lower surface energy phases prefer to precipitate out, whereas higher free energy phases tend to dissolve. In solution, TiO2 growth units are typically plentiful (H. Zhang, and J. F. Banfield, 1999).

In aqueous solutions, Ti(IV) species are octahedrally coordinated by means of vacant "d" orbitals of titanium ions, which enable them to accept electron pairs from nucleophilic ligands such as -OH groups

or H_2O-forming species like $[Ti(OH)n(H_2O)_{6-n}]$ (4-n)+. At elevated temperatures, mononuclear structure will dehydrate and condense, resulting in the formation of amorphous TiO_2 (H. Cheng, 1995).

The kind of ligand that is coordinated to the central titanium depends on the pH of the solution and the existence of species that function as complexing agents. The medium's pH is important even in the absence of complexing organisms. For example, $[Ti(H_2O)_6]^{4+}$ undergoes a stepwise spontaneous hydroxylation to form$[Ti(OH)(H_2O)_5]^{3+}$, $[Ti(OH)_2(H_2O)_4]^{2+}$, $[Ti(OH)_3(H_2O)_3]^{+}$, and [Ti(OH)4(H2O)2]^{0} due to the polarizability of Ti^{4+} ions (H. Zhang and J. F. Banfield, 2000).

These complexes cause the solid phase to develop by generating and growing nuclei through olation and oxolation pathways. Solid phase is likely to result from various zero charge precursors leading to the nucleation of particular polymorph in the presence of complexing agent that can react with co-ordination sphere of cation. On the basis of the "partial charge model," discussions of the production of titania crystal through octahedral connection by corner/edge sharing are common (X. Chen and S. S. Mao, 2007).

(M. Gopal, et al., 1997) Oxolation causes cations to increase linearly along the equatorial plane in the lower pH range if deoxolation does not take place. Rutile is produced from this reaction and the oxolation of the linear chains that arise. As a result of condensation moving in an apical direction during high pH deoxolation, anatase chains can get twisted. According to Henry et al., condensation may be directed toward the cis-skewed chains of anatase .if deoxolation takes place before nucleation.

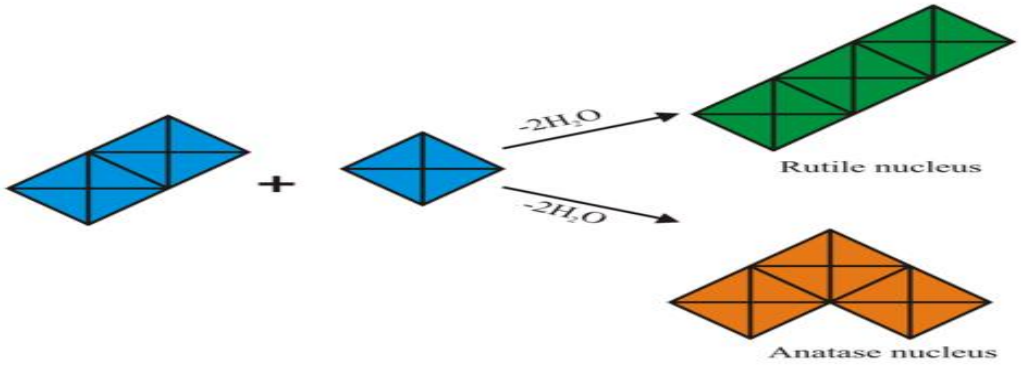

Figure. 2.12: Orientation of third $[TiO_6]$ in linear and zig-zag fashion.
Source: *Nano scale, 2014, 6, 11574*

2.10.2 Phase nucleation depending on solution chemistry

Olation is the process by which metal ions form polymeric oxides in aqueous solution(Hydroxy bridges are formed by nucleophilic substitution, where an OH group attacked and water leaves) .At low PH, many metal ions exist in aqueous solution as aqua coordination complexes, often with the formula $[M(H_2O)_6]^{3+}$,As the pH increases, one O-H bond ionizes to give the hydroxide complex, the conjugate base of the parent hexaaqua complex .

$$[M(H_2O)_6]^{3+} \rightleftharpoons [M(H_2O)_5OH]^{2+} + H^+$$

Metal aquo complexes are coordination molecules in inorganic chemistry that solely have water as a ligand and contain metal ions.The hydroxo complex is about to experience olation, which is started when a nearby complex displaces one water:

$$[M(H_2O)_5OH]^{2+} + [M(H_2O)_6]^{3+} \rightleftharpoons M(H_2O)_5(\mu\text{-}OH)M(H_2O)_5\}^{5+} + H_2O$$

The hydroxide ligand forms a bridge between the two metals in this product; this bridge is indicated by the symbol μ. The leftover water and hydroxo ligands in the resultant 5+ ion are very acidic, allowing the ionization and condensation processes to proceed at even higher pHs. The process of "oxolation," which results in the production of the oxo-dimer .ultimately one observes the formation of the metal oxide (Holleman, A. F. et al., 2001).

$$\{[M(H_2O)_5]2(\mu\text{-}OH)\}^{5+} \rightleftharpoons \{[M(H_2O)_5]2(\mu\text{-}O)\}^{4+} + H^+$$

$$2\,[M(H_2O)_6]^{3+} \rightleftharpoons M_2O_3 + 9\,H_2O + 6\,H^+$$

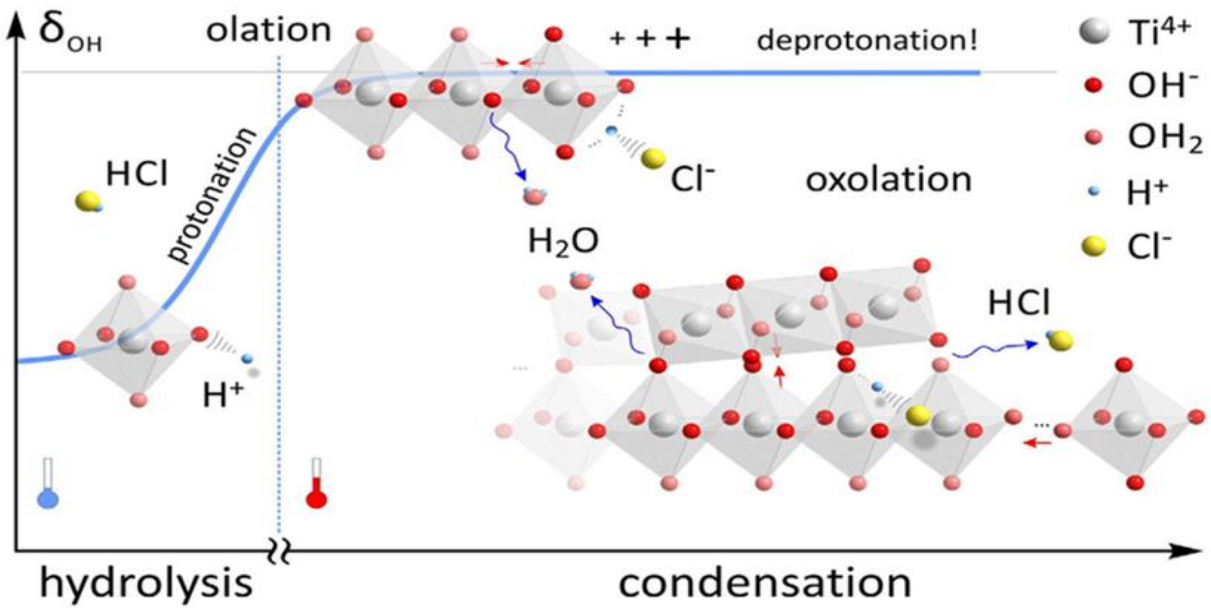

Figure 2.13: Several types of OH bridges can be formed by olation condensation process. Source: *https://www.google.com/url Several-types-of-OH-bridges-can-be-formed-by-olation-condensation-process.*

Ti(IV) species in aqueous solutions are octahedral coordinated, accepting electron pairs from nucleophilic ligands like these by means of the unoccupied "d" orbitals of titanium ions OH group or H_2O-forming species such as $[Ti(OH)_n(H_2O)_{6-n}]^{(4-n)+,}$ where the pH of the medium is a significant factor.$Ti(H_2O)_6$ Stepwise spontaneous hydroxylation of 4+ results in the formation of $[Ti(OH)(H_2O)_5]$. $[Ti(OH)_2(H_2O)_4]^{3+}$ [Ti(OH)3(H2O)3] $^{2+}$ $Ti(OH)4(H_2O)_2$ and + Ti^{4+} ions' polarizability and the nuclei's development via the olation and oxolation pathways (B.-Z. Lin and S.-X. Liu, , 1999).

2.10.3 Manipulating synthesis parameters in favor of rutile phase formation

PH is a very crucial parameter in determining the phase in wet chemical synthesis. In the hydrothermal synthesis of TiO_2, $[Ti\ (OH)_{\ h}\ (H_2O)_{\ 6h}]$ 4h monomers are produced by dissolving the precursor containing titanium ions, and the monomers subsequently undergo a condensation reaction to form TiO_2 crystals. In wet chemical method and Condensation of $[Ti\ (OH)\ n\ (H_2O)_{\ 6n}]^{(4n)\ +} \rightarrow [TiO_6]$ units in TiO_2.

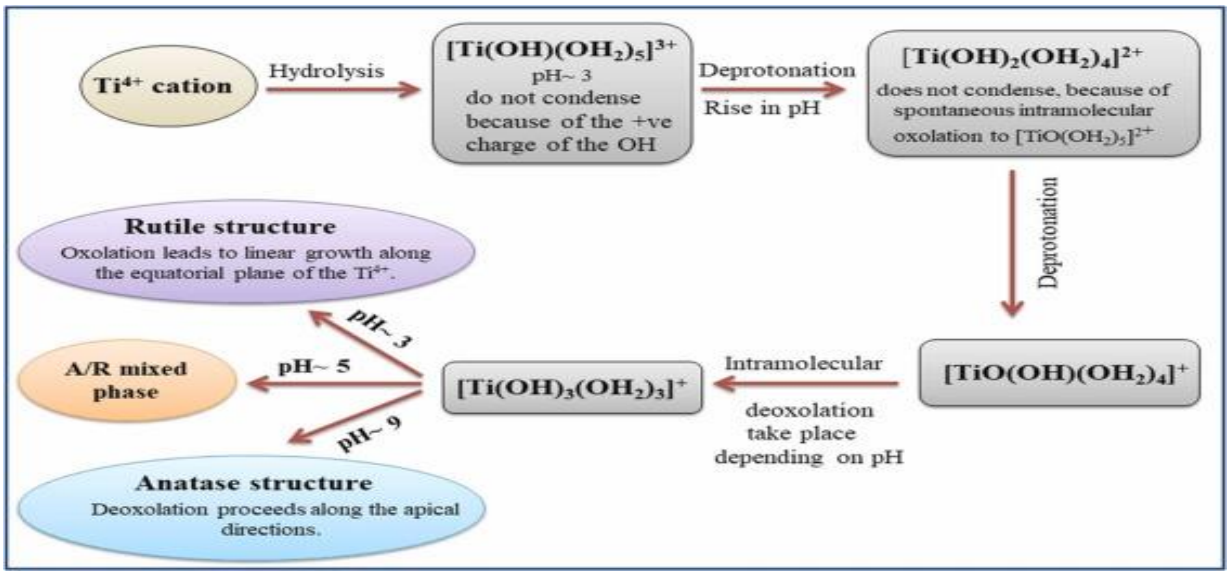

Figure 2.14: Hydrothermal synthesis of TiO_2

Source: *https://www.researchgate.net/profile/Ruediger*

The crystal structure is determined by the hydrolysis ratio, temperature, and PH value. The detailed nucleation process of TiO_2 derived by a $[Ti\ (OH)_h(H_2O)_{6-h}]_{4-h}$ monomer with different hydrolysis ratios, and the corresponding relationship between the hydrolysis ratio and the crystal structure, are based on the principle that the olation reaction occurs before the oxolation reaction.

- At lower pH oxolation occurs during condensation → Rutile
- At higher pH deoxolation occurs → Anatase

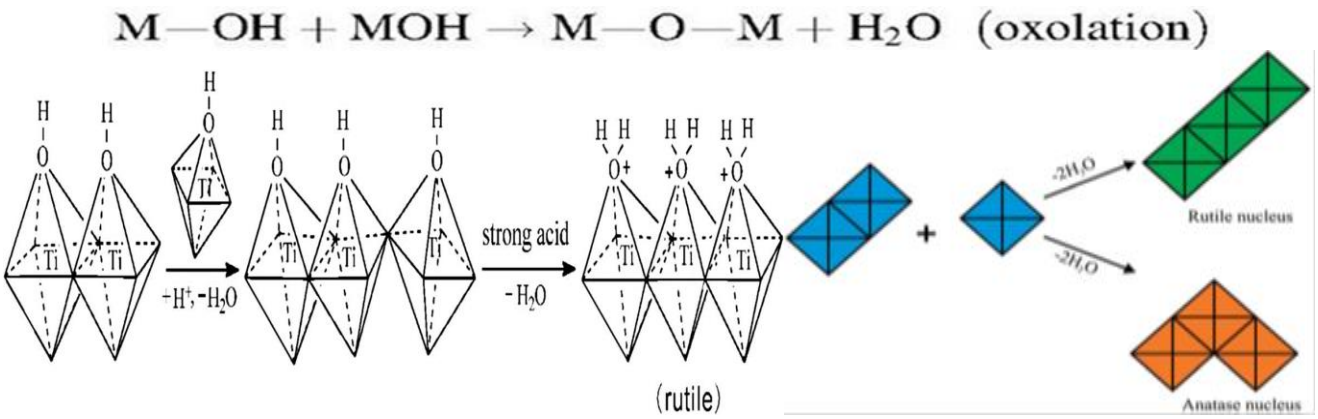

Figure2.15 Orientation of the third $[TiO_6]$ in linear and zigzag fashion

Source: *Nanoscale, 2014, 6, 11574–11632*

2.11 Techniques employed in analysis to examine inorganic layers in effect pigments

(L. Sung, et al., 2000) Light and electron microscopy Light microscopy is an important tool to evaluate the quality of optical layers since it is directly related to the visible color effect, which is the most important attribute the client expects. Techniques that blend bright and dark field are common. Using stray light from the side, the diffuse dark field method is the most effective way to discover internal features of the pigment particles in transparent effect pigments.

The lateral resolution of light microscopy is frequently only half of the illuminating wavelength. Thanks to specialized methods like near-field scanning optical microscopy (NSOM or confocal laser microscopy), the usable resolution has been increased to 50 nm. The thickness of the optical layers usually fall within this range as well. For example, the TiO2 layer of silver-white pearlescent pigments has a thickness of 60 nm(Maile et al., 2005).

2.12 Research Gap

Thermal stress is produced during the thermal processing to crystallize TiO_2 /mica pearlescent as a result of the thermal conductivity mismatch. In the previous finding coating are reported 95% and 100% rutile phase is achieved of by using Pre-coating mica with Rutile directing materials but the coating smoothness becomes worse and optical quality is compromised due to highly rough nature of the rutile coating. In general previous studies show limited mechanical stability in most cases and can, therefore, not be used in technical applications where stress is exerted.

Thermal stress causes the TiO_2 coating to break, which causes light scattering and causes the pigment's optical quality to degrade. TiO_2 was applied to mica substrates that had already been prepared using the titration approach and the heterogeneous nucleation process. Mica is a mineral extracted from earth's crust thus consists of different cations (Si^{4+}, Al^{3+},Mg^{2+}, k^{+}) than alumina (Al^{3+}) which can diffuse in to TiO_2 structure and interfere in the anatse to rutile phase transformation process .One alternative is to use a smooth surface substrates and synthetic method that allows for low-temperature crystallization.

The other alternative to control the coating smoothness is controlling the hydrolysis kinetics of TiO_2 from its precursors. The hydrolysis kinetics of TiO_2 precursors is dependent on several factors such as reaction temperature, pH of the synthesis media, and the likes. Since pH has a profound effect on the

hydrolysis kinetics, it is better to keep the pH of the synthesis media uniform throughout the solution. The problem associated with the common pH controlling mechanism in the TiO_2 coating, which is drop wise addition of acids or bases, is the occurrence of local pH variation which causes different hydrolysis kinetics and thus non uniform coating. In this research, we are trying to address coating smoothness issues and the crack formation in the coating using in-situ urea decomposition as a pH controlling agent and pH control as a means of obtaining high rutile phase fraction at lower temperature.

3. MATERIALS AND METHODS

The experimental works were conducted in the laboratory of Addis Ababa science and Technology University and leather and leather product research and development center (LLPRDC) Addis Ababa, Ethiopia and sample Characterizations such as surface area analysis of the Alpha alumina were performed at Bahirdar University, Ethiopia. SEM, XRD and UV-Vis/NIR and The color index of the pigments analysis were done at central Research Laboratory of Korea Advanced institute of Science and Technology (KAIST), South Korea.

3.1 Materials

In This study Electronic balance was employed in order to take weight measurements .Ball mill has been used to mix the precursor powders of alumina synthesis and box furnace is used to carry out the alumina synthesis reaction. Beakers of size 1l were used to carry out the washing out of the salt mixtures from the product of the alumina synthesis procedure. PH meter (Schott AG, Mainz, Germany) was used to perform acidity and/or basicity of the sample. Beaker of size 100ml were used to carry out the co-precipitation of oxy-sulfate, hot plate with magnetic stirrer has been used to facilitate the temperature control and uniform mixing of the co-precipitation reaction. Eclectic Oven has been used for drying samples. During the process the separation of liquid and solid was performed by using filter paper (whatman and nano filter).

Morphology of the synthesized samples has been analyzed using field-emission scanning electron microscope (FESEM; XL 30, Philips, The Netherlands). To analyze the phase of the synthesized powders X-ray diffractometer (Rigaku D/Max-RB) with CuKa radiation (l = 1.5418 A˚) has been used. Surface area analysis has been done using Brunauer–Emmett–Teller (BET) surface area analyzer (Autosob iQ-x). UV-Vis/NIR spectro photometer (Cary 500, Varian Inc., CA, and USA) and the color index of the pigments has been analyzed using colorimeter (WPA, C07500).

3.2 Chemicals

All chemicals and reagents used in this study are aluminum hydroxide ($Al(OH)_3$) (99%, Sigma Aldrich), $Na_2(SO)_2$ (99%, Sigma Aldrich), $K_2(SO)_4$ (99%, Sigma Aldrich) as substrates for synthesizing Alumina.

Titanium oxy-sulfate ($TiOSO_4.2H_2O$, 99% Pure, Sigma Aldrich) is used as a precursor for TiO_2 synthesis and urea (CH4N2O, 98%, Sigma Aldrich) is used and commercial mica.

Research design

Research design follows according to chart below:

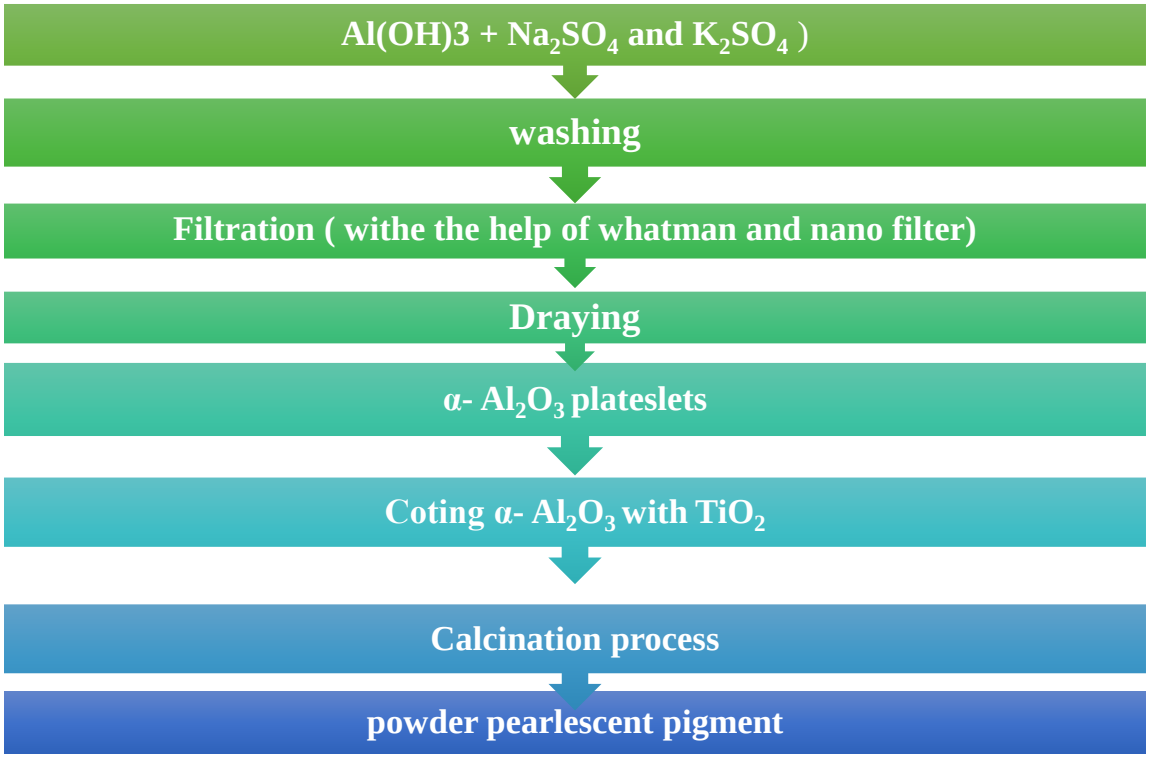

Figure 3.1: Process flow of α- Al_2O_3 with TiO_2 pearlescent pigment

3.3 Methods

3.3.1 Alpha alumina synthesis

Alpha alumina is synthesized using molten salt synthesis technique (Li-Hui & Qing-Wei, 2011).The precursor $Al(OH)_3$ is mixed with eutectic composition (20 mole % Na_2SO_4) of Na_2SO_4 and K_2SO_4 salt mixture using ball mill. The mixture salts are more beneficial to the development of α- Al_2O_3 platelets than pure salt (Li-Hui & Qing-Wei, 2011), and are preferable to pure salt for the conformation of α-Al_2O_3 platelets. Wet milling of the powder mixtures was done using ethanol as a liquid media, for about 12h.

The slurry from the ball mill was poured in to a beaker and heated to 80^{o}C while stirring until all the ethanol was evaporated. The semi dried powder was taken from the beaker and kept in an oven at 100^{o}C overnight. The dried powder was then placed in to crucible and then heat treated in a box furnace at 1100^{o}C for 4h. Finally, the heat treated sample has been washed several times until the salt mixture is removed from the product. α- Al_2O_3 platelets were prepared according to the flow chart shown in Fig.3.1.

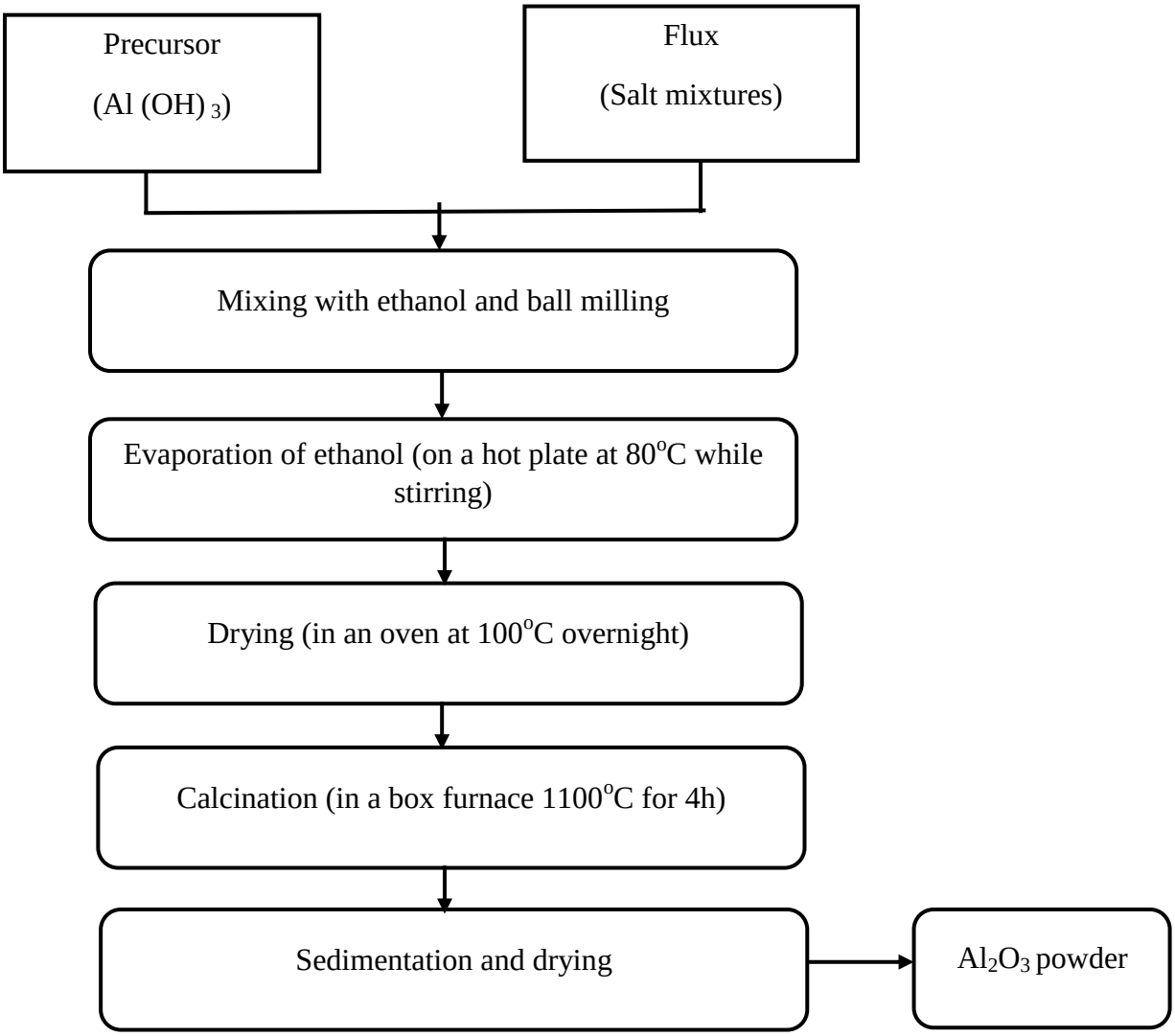

Figure 3.2: Process flow of α- Al_2O_3 synthesis

The cooling process affects both the number of nuclei and the size of the final crystals of alpha alumina in the process, controlling the cooling rate is crucial to the formation of single crystals. Because a large number of particles are present before cooling and the sample dissolved in the molten salt precipitate on the surfaces of the already-existing solid particles, the cooling rate has no effect on the sizes of the particles in the synthesis of molten salt. The synthesizing of alpha alumina was conducted in the laboratory of leather and leather product research and development center of Ethiopia.

Figure 3.3: Process fellow of synthesizing process of Alpha alumina

3.3.2 TiO_2 coating

TiO_2 coating was made using co-precipitation technique (Hyoung & Zuo, 2004) 2.5g alpha alumina was suspended in 100ml deionized water under constant stirring. 15 wt% titanium oxysulfate in sulfuric acid was used as a precursor for TiO_2 coating. $TiOSO_4$ solution in a molar ratio of 1:10 with alumina substrate

was added to the alumina suspension. To control the pH thus the hydrolysis kinetics of the $TiOSO_4$ urea at a molar ratio of 5:1, 25:1, and 50:1 with $TiOSO_4$ was added to the suspension. Urea is selected in this study since it can decompose and release ammonia uniformly which in turn controls the pH of the synthesis media without local pH variation and thus facilitates the uniform coating process.

The urea: $TiOSO_4$ ratio was predetermined in a separate experiment to make the pH of the synthesis media at acidic (pH~1), neutral (pH~7) and basic (pH~11) conditions respectively. The reaction mixture is slowly heated to 90^oC and kept at that temperature for 5h to ensure a complete urea decomposition and $TiOSO_4$ hydrolysis. After the reaction was completed the mixture was kept on the hot plate without steering and heating until it cools down to room temperature and the mixture is settled down. Once the mixture is settled the supernatant is decanted and the sediment is washed several times with DI water until the pH of the supernatant after washing becomes neutral. The washed sample is then dried in an oven at 100^oC overnight.

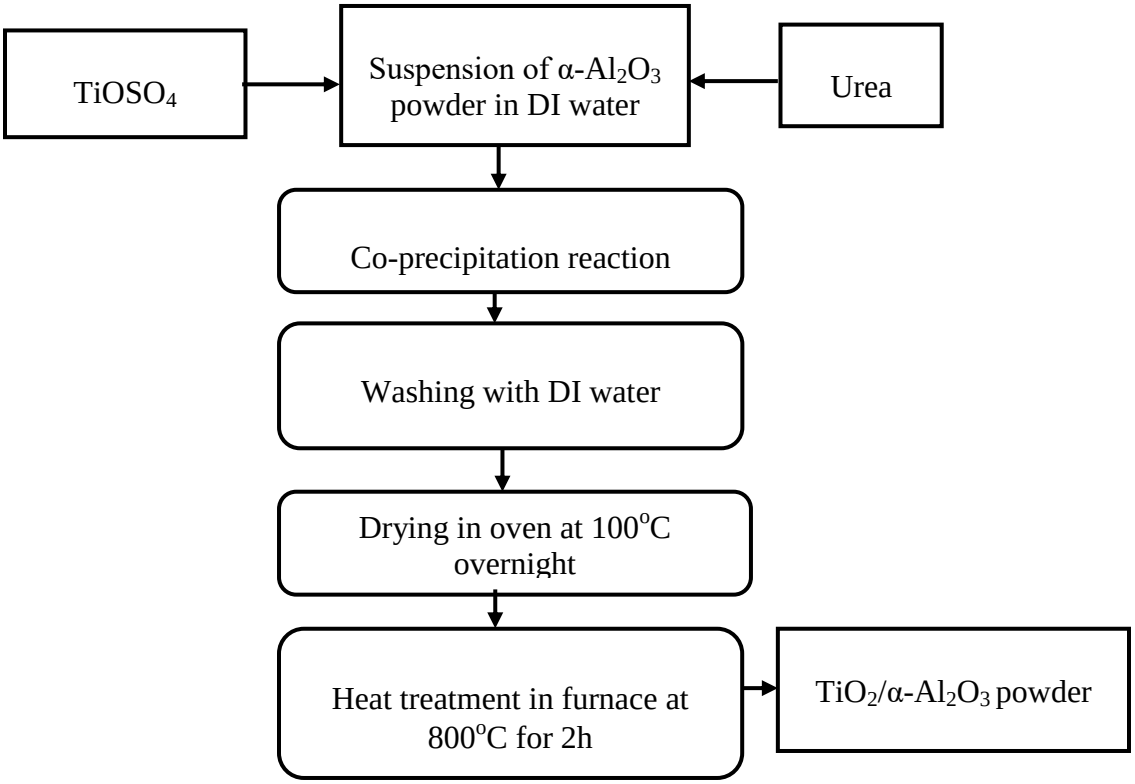

Figure 3.4: Process flow TiO_2 coating on α-Al_2O_3 powder

3. 4 Design expert with RSM

Surface response method (RSM) used for optimization of the synthesis parameters. The RSM method that assesses the correlation between components (X1, X2, and X3), and experimental outputs, or responses. Typically, this approach is combined with factorial design method such as central-composite designs. By using this design, compared to conventional factorial design methods, the number of experimental sets can be drastically decreased without decreasing the optimization accuracy (Q. Zhao et al). The results obtained from the experiment were analyzed with ANOVA (analysis of variance) to model the relationship between various factors and the responses. The three variables studied for the preparation of titanium oxide were concentration ratio, temperature and time as summarized below.

Table3. 1: The levels used for concentration, temperature and time

Factor		Level		
		1	0	-1
X1	Concentration (gl^{-1})	5	25	50
X2	Temperature (°C)	200	500	950
X3	Time (h)	1	2	3

The central composite design with RSM is used in the discovery to provide a model to characterize the relationships that take interaction effects of each fators.in his study this method was used into account and allow us to forecast and regulate the phase transformation under various conditions. Secondly, using the response surface, the influencing tendency of each factor is explored. Finally, the optimal conditions are determined for engineering use. According to the design expert the three factor interaction and run automatically analyzed on table 3.2.

Table3. 2: Different parameters to evaluate the Color value (whiteness)

Std	Run	Factor 1 A:temperture (˚C)	Factor 2 B:Concenteration (gm/l)	Factor 3 C:time (hr)
19	1	500	27.5	1.5
17	2	500	27.5	1.5
16	3	500	27.5	1.5
9	4	950	27.5	2
11	5	500	30	1.5
20	6	500	27.5	1.5
6	7	800	5	2
18	8	500	27.5	1.5
2	9	800	24.5	1
15	10	500	27.5	1.5
13	11	950	27.5	3
8	12	800	50	2
5	13	200	5	2
4	14	950	50	1
12	15	500	50	1.5
1	16	200	5	1
10	17	950	27.5	3
3	18	200	50	1
7	19	800	5	2
14	20	950	27.5	2.3409

This method analyzes the model significance and the response result automatically. The RSM result that was covered in the section on results and discussion. Differentiating the temperature, concentration, and time allowed for the analysis of the phase and particle size changes that occurred during heating. The field-emission scanning electron microscope was used to characterize and observe in real time the changes in particle shape and phase transition that occurred during the heating process.

3.5 Particle size measurement:

The average particle size of the synthesized alumina and the commercial mica are analyzed using several SEM images and an image analysis software called image-J. About 100 particles from different SEM micrographs in which clear particle measurement can be made are used to measure the particles. The average size of the 100 particles and the corresponding standard deviation is presented as the particle size of the powders.

3.6 Rutile phase fraction calculation

The rutile phase fraction was calculated using equation 3.1 below with the (110) peak of rutile and the (101) peak of anatase. X-ray diffraction patterns of TiO_2/substrate pearlescent pigments were recorded to determine the phase of TiO_2. The percentages of rutile and anatase in TiO_2 layer were calculated from X-ray powder diffraction intensities (M.A. Barakat et al., 2005).

$$X_R = \frac{1}{1+0.8I_A/I_R} \quad \text{.....3.1}$$

Where: $X_R$is rutile phase fraction, I_A is intensity of 100% anatase peak, and $I_R$is intensity of 100% rutile peak.Where IA and IR are the integrated intensities of anatase (1 0 1) reflection and rutile (1 1 0) reflection, respectively.

3.7 Sample characterization

The phases of synthesized alumina powder and the TiO_2 coated samples are done using high-resolution X-ray diffractometer (XRD; Rigaku D/Max-RB, 12 kW, Japan) with Cu Kα radiation (λ = 1.5148 Å) operating at 40 kV and 300 mA at central Research Laboratory of Korea Advanced institute of Science and Technology (KAIST), South Korea. The morphology of the synthesized samples is analyzed using Field-emission scanning electron microscope (FESEM; XL 30, Philips, The Netherlands) at the Central Research Laboratory of KAIST. The surface area of the synthesized alumina and commercial mica were analyzed using BET (Brunauer, Emmett and Teller, Model ASAP 2010, Micrometrics Co., Norcross, GA) surface area analyzer at Bahirdar University, Ethiopia. The optical quality of the pigments was analyzed using a UV-Vis/NIR spectrophotometer and Colorimeter.

3.8 Experimental instruments used on the research work

3.8.1 Brunauer–Emmett–Teller (BET) measurement

BET used to measure the surface area of solid or porous materials. It gives important information on their physical structure as the area of a material's surface affects how that solid will interact with its environment. The surface area of the synthesized α-Al_2O_3 has been analyzed by using Brunauer–Emmett–Teller (BET) surface area analyzer (Autosob iQ-x).

3.8.2 Scanning electron microscopy (SEM) test

In this study scanning electron microscope is used to create an image by scanning a specimen's surface with an electron beam inside of a vacuum chamber. Alpha alumina substrate topography is characterized, and it also analyzes the surface aspects of the material, or "how it looks," as well as the texture and the relationship between these qualities and the material's properties. In this research, surface smoothens; particle size and shape, and substrate morphology are all examined. There is a direct correlation between these structures, the qualities of the materials, and the crystallographic data obtained from the sample by scanning electron microscopy. The investigated samples were characterized by field-emission scanning electron microscope (FESEM; XL 30, Philips, The Netherlands).

3.8.3 X-ray diffraction (XRD) test

X-ray diffraction is a common technique that determines a sample's composition or crystalline structure. It is used to determine the structure of atoms within the sample. Helps to find the crystal size and it can determine sample composition and also phase purity. The result of X-ray diffraction plots the intensity of the signal for various angles of diffraction at their respective two theta positions. A thinner peak corresponds to a bigger crystal. A broader peak means that there may be a smaller crystal and if it has the same phase pick intensity as the reference pattern the result shows good crystallites(Fatimah et al., 2022). In this study the investigated synthesized sample of alpha alumina and coated sample crystal structure was characterized by X-ray diffractometric analysis high-resolution X-ray diffraction (XRD; Rigaku D/Max-RB, 12 kW, Japan) with Cu Kα radiation (λ = 1.5148 Å) operating at 40 kV and 300 m used.

3.8.4 UV/VIS/NIR spectroscopy test

UV-Vis spectroscopy test is used for the investigation of the optical properties of the pigments (D65 illuminant). The technique measures the absorption of light across the desired optical range. A sample is dispensed into a cuvette and placed in the path between the optical light source and a detector. According to the Beer-Lambert law, with a constant light path length and known absorption coefficient (dependent upon wavelength), the concentration of a compound in question can be determined from the light absorbed at that wavelength. A sample is placed in front of the integrating sphere and light from an optical light source is transmitted through the sample and enters the integrating sphere. The light is then reflected by the internal surface of the sphere and reaches the detector. Both the overall transmittance and the direct transmittance can be measured.

The absorbance percentage is defined as the percentage of the incident beam absorbed by the sample i.e. that neither part of the beam which is neither reflected nor transmitted. Absorbance can be calculated from the reflectance and transmittance. In the study the investigated sample absorbance calculated by UV-Vis/NIR spectro photometer (Cary 500, Varian Inc., CA, USA).the finding in high optical quality without occurrence of cracking is the main target the research part and the result is shown in chapter four.

3.8.5 Color index measurement

The color index of the material measured by colorimeter. It refers to a device which helps specific solutions to absorb a particular wavelength of light. The science of connecting color to human perception is called colorimetry (Doreen Becker, in Color Trends and Selection for Product Design, 2016). To measure light and link it to the X (red), Y (green/yellow), and Z (blue) components of CIE 1931 color space, An additional method to relate color on the L*a*b* color space to human vision. With a numerical range of 0–100, where the lightest (or whitest) color is equal to 100 and the darkest (or darkness) color is equal to zero, the L* value describes the brightness of a color.in the investigation the color index of the pigments have been analyzed using colorimeter (WPA, C07500).

3.9 Data collection

3.9.1 Secondary data

This study uses literature reviews to refer the Surface coating of different substrates with TiO_2 nano-particles for special effect (pearlescent) pigment. Different secondary sources will use regarding TiO_2 coating and its processing parameters.

3.10 Method of Data Analysis

The results of the laboratory experiments were summarized and discussed using tables, figures, and pictures and Response surface methodology (RSM), which is based on factorial design, is a mathematical and statistical technique for designing experiments, fitting models, and determining the optimal operating conditions for a target response in the chapter four. The findings were interpreted into viable meanings by using discussion made on previous research findings.

4. RESULTS AND DISCUSSION

4.1 Characteristics of the synthesized α-alumina

The synthesized nanoparticles are pure α-Al_2O_3 nanoparticles with high degree of crystallinity as can be observed from XRD pattern of the synthesized powder on Figure 4.1, which exactly matches the standard reference pattern of the α-Al_2O_3 crystalline phase. Figure 4.2(a and b) demonstrates the SEM image of the synthesized α-Al_2O_3 and commercial mica respectively. As can be observed from the SEM images, the synthesized α-alumina nanoparticles are flaky shaped with smooth surface. The surface of α-Al_2O_3 particles have a relatively flat surface whereas the surface of commercial mica looks to have more uneven surface. α-alumina nanoparticles have better surface smoothness than the commercial mica. Surface smoothness of the substrate has a positive effect on the pearl like luster of the final pigment as it favors homogeneous nucleation and consequent smooth coating(Grosfils & Lutsko, 2021).The average particle size of the synthesized α-alumina is ~10μm and that of commercial mica is ~5μm(Gao et al., 2012).The higher particle size of α-alumina is also an advantage to the optical quality of the final pigment as the increment in particle size reduces the proportion of light scattering form the age of the particles compared to those reflected form the interface.

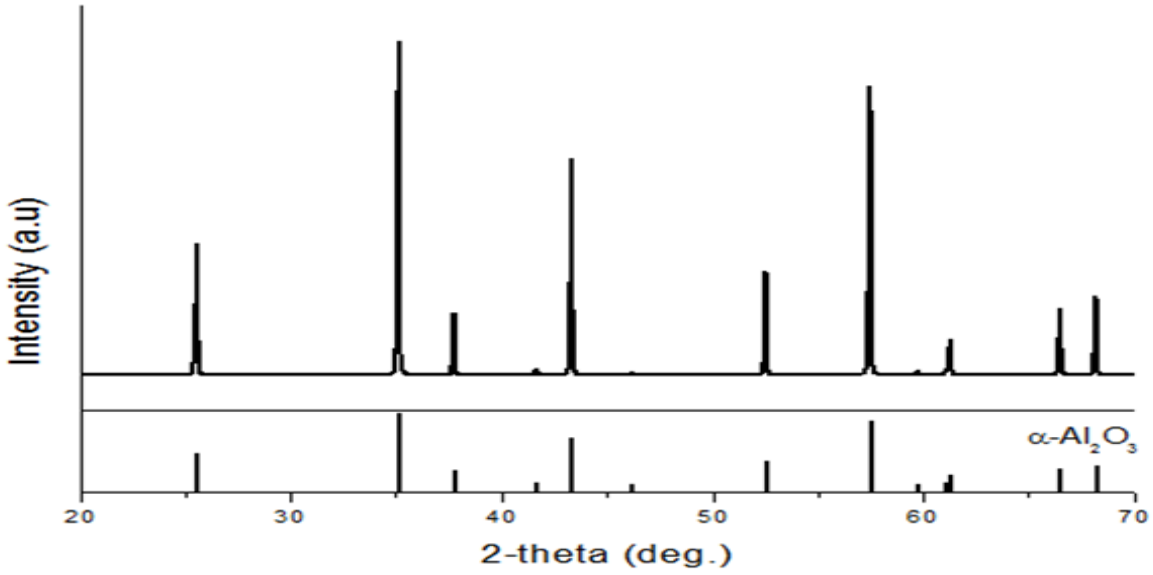

Figure 4.1 XRD pattern of the synthesized powder

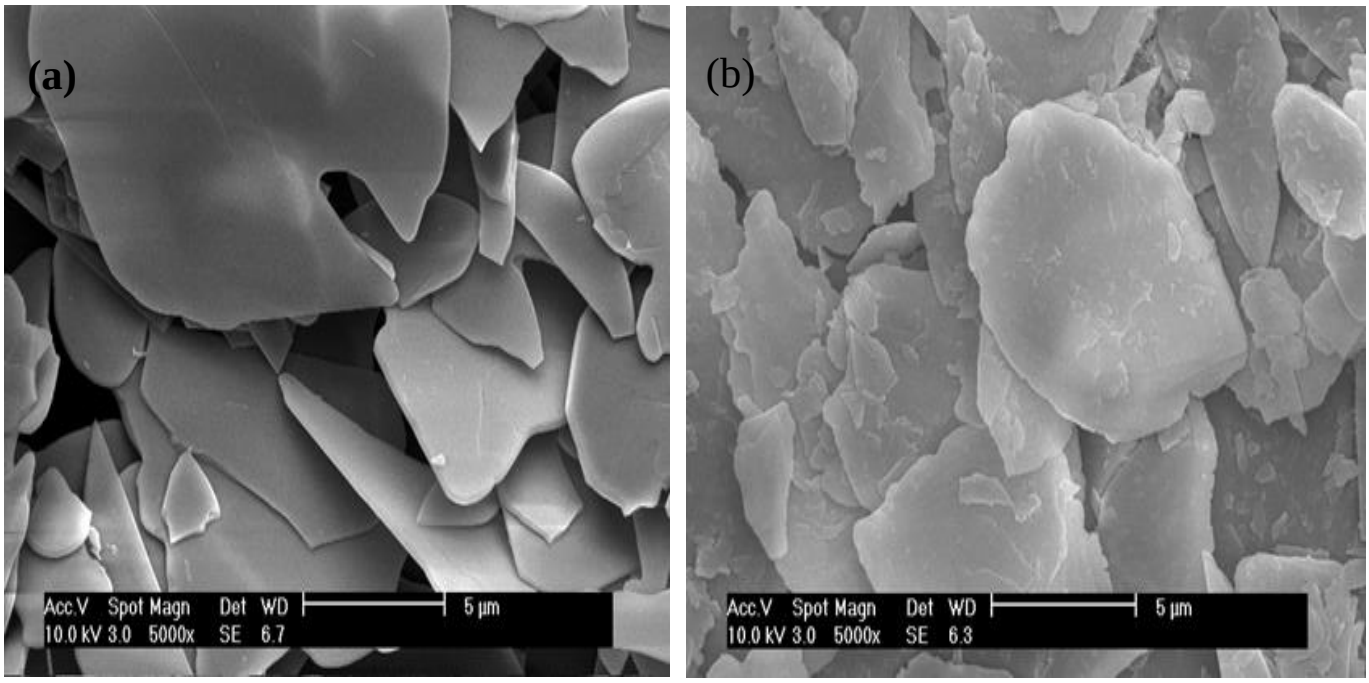

Figure 4.2 SEM images of: (a) synthesized α-Al_2O_3 powder, (b) Commercial Mica powder

The surface area of the synthesized α-Al_2O_3 is lower than that of the commercial mica, as can be observed from Table 4.1.(Grosfils & Lutsko, 2021)the higher surface area of mica could be attributed to the higher surface roughness and the smaller particles size of the commercial mica compared to that of α-Al_2O_3.

Table 4: 1 Surface area and average particle size of synthesized α-Al_2O_3 and commercial mica

	BET (Surface area)	**Average particle size(µm)**
Mica	11.0416m^2/g	~5±3.5
α-Al_2O_3	2.1902m^2/g	~10±7.2

4.2 Statistical Analysis of the Experimental Results

This study employed Design-expert software 13 and RSM based on Central composite design to examine the effects of temperature, time, and concentration ratio on the preparation of alpha alumina/titan pearlescent pigment. ANOVA was used to examine the model's statistical significance, as indicated in table 4.2.

Table 4: 2 Analysis of variance results for acquired mode

Source	Sum of Squares	Degrees of freedom	Mean Square	F-value	p-value	Characteristics
Model	9175.28	3	3058.43	31.67	< 0.0001	Significant
A-temperature	7346.51	1	7346.51	76.07	< 0.0001	Significant
B-concentration	0.7598	1	0.7598	0.0079	0.0045	
C-time	35.30	1	35.30	0.3655	0.0039	
Residual	1545.23	16	96.58			
Lack of Fit	1223.92	8	152.99	3.81	0.0381	Insignificant

$R^2 = 0.8559$; Adj-$R^2 = 0.8288$

The model is deemed significant based on its F-value of 31.67. Noise has a mere 0.01% probability of producing a "Model F-Value" of this magnitude. Model terms are considered significant when P-values are less than 0.0500. A is a significant model term in this instance. The 3.81 F-value for lack of fit indicates that the lack of fit is not substantial. In relation to the pure mistake. A solid indicator that the aforementioned model is suitable for predicting the range of variables under study is the non-significant

lack of fit. A, B, and C are important model terms in this instance. The model terms are not important if the value is bigger than 0.1000.

Table 4: 3 R-squared (R^2) value for the model

Fit Statistics			
Std. Dev.	9.83	R^2	0.8559
Mean	60.47	Adjusted R^2	0.8288
C.V. %	16.25	Predicted R^2	0.8097
		Adeq Precision	15.2708

There is less than 0.2 discrepancy between the "Adjusted R^2" of 0.8288 and the "Predicted R^2" of 0.8097, indicating a reasonable agreement."Adeq Precision" calculates the ratio of signal to noise. Ideally, the ratio should be higher than 4. "An adequate signal is indicated by your ratio of 15.271."

The statistical summary produced by Design Expert 13 for each model is displayed in Table 4.4. Despite having lower R^2 and adjusted-R^2 (Adj-R^2) values than a quadratic and cubic model, a linear model was proposed. As a result, the impacts of every variable that generates a separate signal blend together.

Table 4: 4 Statistical summaries for each model

Source	Sequential p-value	Lack of Fit p-value	Adjusted R^2	Predicted R^2	
Linear	< 0.0001	0.0381	0.8288	0.8097	Suggested
2FI	0.7075	0.0188	0.8100	0.6350	
Quadratic	0.0934	0.0328	0.8662	-2.5548	
Cubic	0.0328		0.9288		Aliased

Model fitting and analysis of variance (ANOVA) Experiments were performed using the centered composite RSM experimental design. The result shown along with the experimental conditions in the above table shows the coefficient of determination (R^2) is defined as the ratio of the explained variation to the total variation, and is a measure of the degree of fit. (Joglekar et al., 1987) Suggested that a good model fit should yield an R^2 of at least 0.8. This means that the response model evaluated in this study can explain the reaction very well, with an R^2 of 0.8559and and Adj-R^2 of 0.8288 at a confidence level of 95%. In addition, the model is very significant, as is evident from its F-value (F model = 31.67) and very low probability value (p = 0.0001). A p-value lower than 0.05 indicates that the model is statistically significant, whereas a value higher than 0.1000 indicates that the model is not significant.

4.3 Results of the coating experiments

Coating of TiO_2 on the surface of the synthesized α-Al_2O_3 have been done using co-precipitation technique. Titanium oxy-sulfate has been used as a precursor. The hydrolysis of oxysulfate is highly affected by pH of the synthesis media. Ammonia obtained from in situ urea decomposition has been used to control the pH of the synthesis media. The pH is controlled by varying the ratio of urea to oxysulfate.

Figure 4.3 and Figure 4.4 demonstrates the morphologies and phases of the resulting powders after the coating experiments at three different urea to oxysulfate ratio.

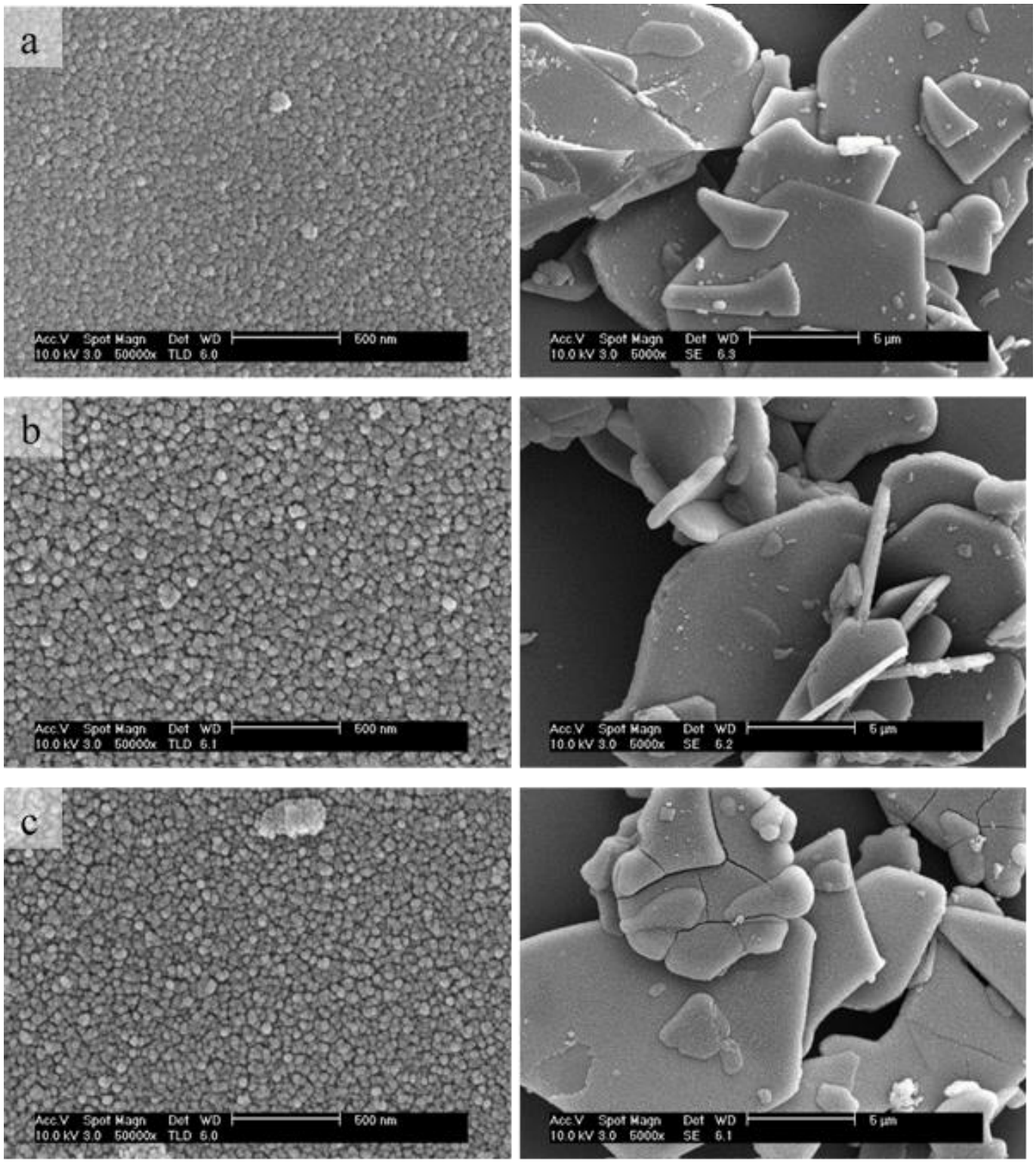

Figure 4.3: Higher and lower magnification images of as coated α-Al_2O_3 powders: (a) at 1:5 oxysulfate: urea molar ratio, (b) 1:25 oxysulfate: urea molar ratio, and (c) 1:50 oxysulfate: urea molar ratio

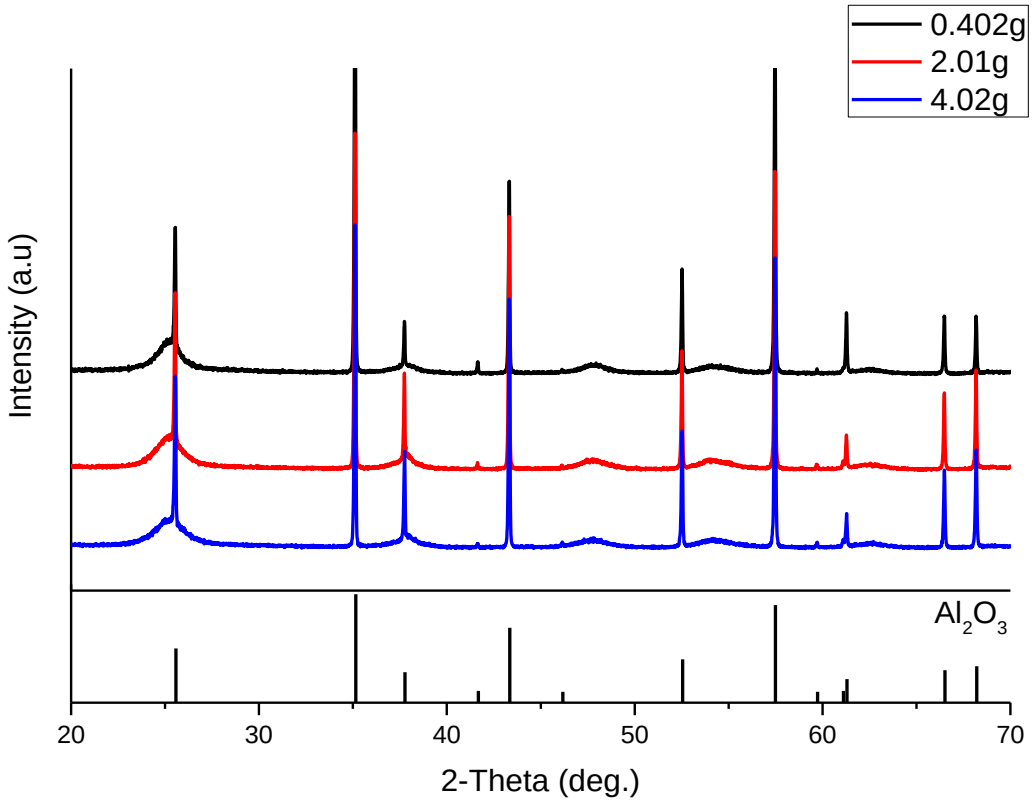

Figure 4.4: The XRD patterns of the as coated α-Al_2O_3 powders at different urea concentration

As can be observed from Figure 4.3, the surface coatings for all the three cases are smooth and uniform. In all the three cases, 25-50nm size granules uniformly coated the entire surface α-Al_2O_3 particles. The smooth coatings are the good manifestation of the effectiveness of pH control using in-situ urea decomposition in resulting uniform hydrolysis of the oxysulfate. The common way of controlling the pH of the reaction media using drop wise addition of acidic and basic solution usually creates local pH variation, which in turn creates variation in the hydrolysis kinetics of the precursor resulting in inhomogeneous coating.

The good surface smoothness of the substrate α-Al_2O_3 particles has also contributed to the uniformity of the surface coating as it avoids preferential nucleation sites, which leads to inhomogeneous coating. The phases of the coated nanoparticles are amorphous as can be observed form Figure 4.4. Only broader humps, which indicate lack of crystallinity, are observed on all the XRD patterns except the sharp peaks corresponding to the crystalline α-Al_2O_3. This is a common phenomenon in all hydrolysis products of

TiO_2 precursors before heat treatment. (Gao et al., 2012)According to previous studies, the hydrolysis of TiO_2 precursors result in hydrated titania (Ti (OH) $_4$) which is amorphous. To get crystalline TiO_2, further heat treatment is usually needed. After the oxysulfate is hydrolyzed in to hydrated titania the remaining component becomes sulfuric acid which will be added up to the already existing sulfuric acid solution in the original oxysulfate solution(Grzmil et al., 2014).

The hydrolysis products do not show any significant phase and morphology change on the coated nanoparticles in all the three cases. Thus, the effect of the pH variation on the phase and morphology of the final coating could not be apparent on the as coated powder.

The coated α-Al_2O_3 particles further heat treated at 800^{o}C for two hours. The heat treatment temperature is selected by optimizing the rutile phase fraction with the pigment quality. The phases and morphologies of the heat-treated samples are presented on Figure 4.5 and Figure 4.6 respectively.

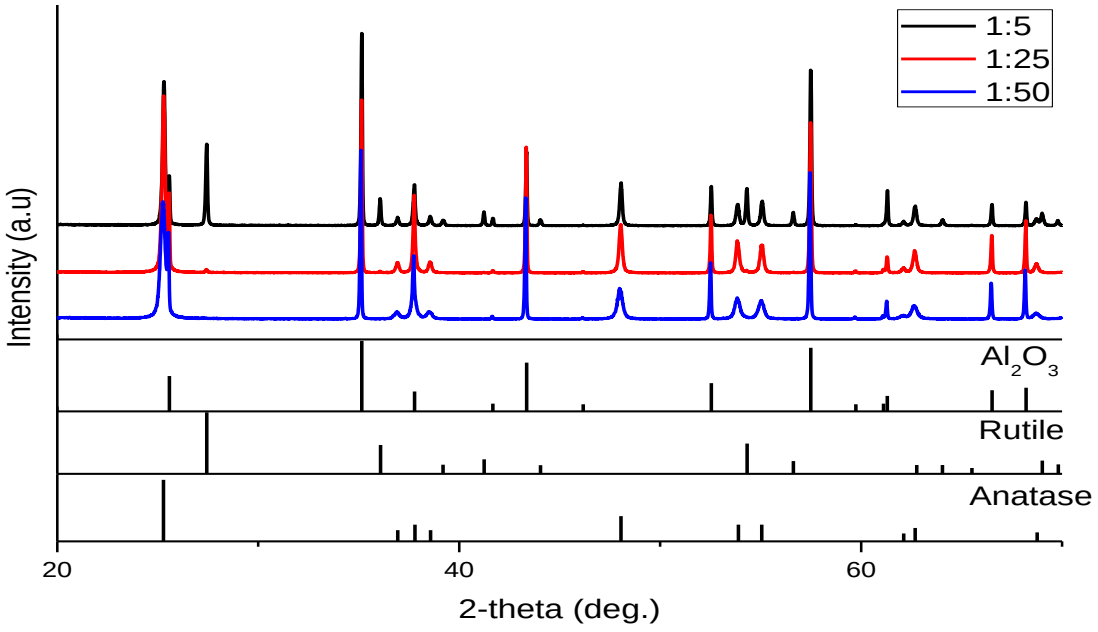

Figure 4.5: The XRD patterns of heat-treated TiO_2/α-Al_2O_3 powders at different oxysulfate/urea ratio

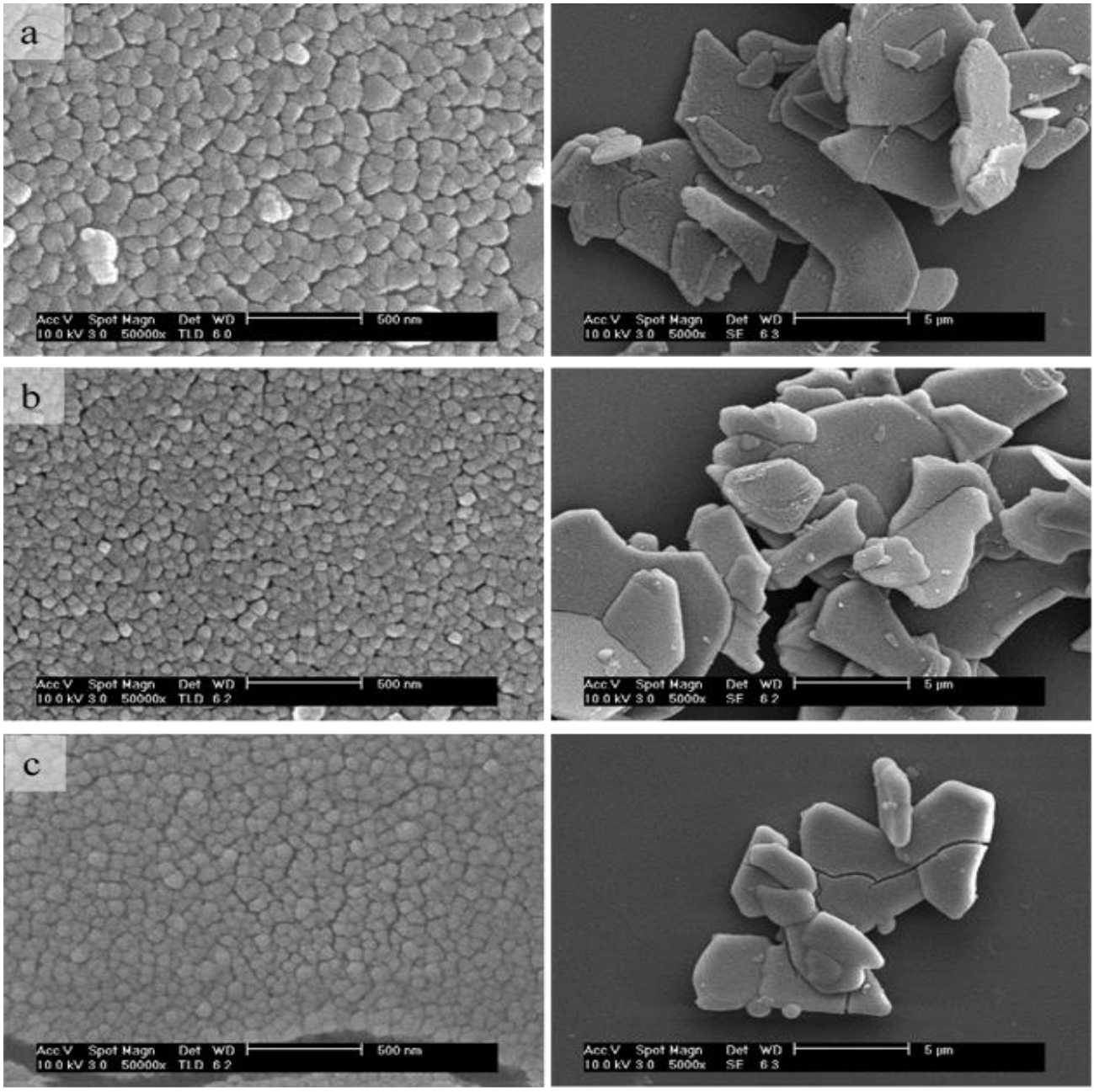

Figure 4.6: Higher and lower magnification images of heat treated TiO_2/α-Al_2O_3 powders: (a) at 1:5 oxysulfate: urea molar ratio, (b) 1:25 oxysulfate: urea molar ratio, and (c) 1:50 oxysulfate: urea molar ratio

XRD patters on Figure 4.5 demonstrate that the amorphous phases of the as coated samples completely converted to different crystalline phases in all the three samples after heat treatment. All the three samples revealed XRD peaks corresponding to the crystalline phase's α-Al_2O_3, anatase TiO_2, and rutile TiO_2. However, there is an observable difference in relative intensity of rutile to anatase phases in the three samples. As the oxysulfate to urea molar ratio decreases (i.e. reaction media goes from acidic to basic pH), the relative size of the 100% rutile peak (Figure 4.6) becomes smaller indicating the rutile phase fraction of the samples decrease with increase in pH.

Quantitative analysis of rutile phase fraction of the heat treated TiO_2/α-Al_2O_3 powders has been made using equation 3.1:

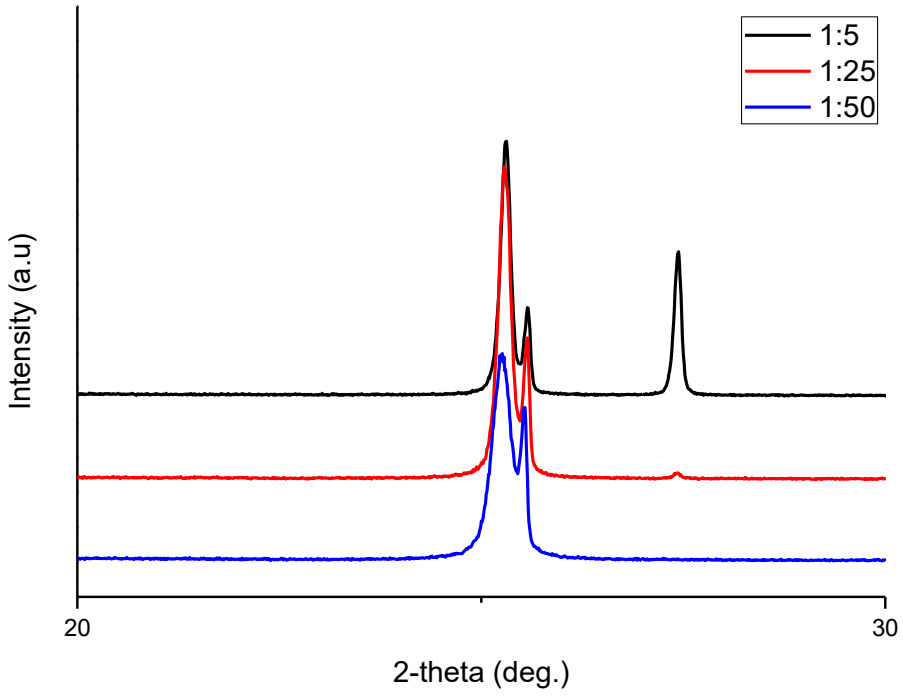

Figure 4.7: portion of the XRD patterns of the heat-treated TiO_2/α-Al_2O_3 where 100% rutile and anatase TiO_2 peaks belong

The rutile phase fraction of the heat-treated TiO_2/α-Al_2O_3 powders for the three different samples, as calculated by equation 3.1, are presented in Table 4.2 below:

Table 4: 5 Rutile phase fraction

Oxysulfate:urea	**1:5**	**1:25**	**1:50**
% Rutile	41.5	2.9	1.4

Table 4.5 indicates that there is significant difference in rutile phase fraction among the samples synthesized at different oxysulfate:urea ratio after heat treatment. The sample with lower oxysulfate:urea ratio (i.e. strongly acidic synthesis media) resulted in higher rutile fraction (41.5%) while the other two samples, where the oxysulfate:urea ratios are 1:25 (i.e. close to neutral pH) and 1:50 (i.e. strongly basic synthesis media), resulted in extremely lower rutile phase fraction, 2.9% and 1.4% respectively

The result indicates that the pH of the synthesis media has effect on how the growth unit combines to yield a particular crystalline phase. Studies indicated that during condensation of $Ti(OH)_4$ to yield TiO_2, the way the growth units (TiO_6) combines to yield TiO_2 is affected by the pH of the synthesis media. In acidic environment, oxolation leads to linear growth along the equatorial plane of the cations. The resulting combination of growth units by corner sharing yields linear chain which favors rutile phase formation. On the other hand, at higher pH values, when deoxolation takes place, condensation can proceed along apical directions and leads to the skewed chains, where the growth units combined by edge sharing, consequently favoring the anatase structure (M. Gopal, et al., 1997).

Thus, it was possible to obtain higher rutile phase fraction just by manipulating the synthesis condition, without employing extremely higher temperature to induce the phase transformation. The above result shows high rutile phase fraction with relatively low temperature and for short period of heating time compared to other finding (Gao et al., 2012) and (Topuz et al., 2011).

The high and low magnification images of the heat treated samples, as can be seen on Figure 4.6, shows smooth surface coating with no apparent crack formation. This indicates that the relatively lower heat

treatment temperature for a short period of time did not cause any significant thermal expansion mismatch between the substrate (Alumina) and the coated TiO_2 which can induce significant strain and consequent crack formation.

4.4 Statistical Analysis of the Experimental Results of Color value

RSM based on Central composite design was used to investigate the effect three factors on Color value (whiteness**)** of synthesized alpha alumina/titan pearlescent pigment.

Table 4: 6 Different paramenter to evalute the color absorbance test

Run	Factor 1 A:temperture(˚C)	Factor 2 B:Concenteration(g m/l)	Factor 3 C:time(hr)	Color value (whiteness)
1	500	27.5	1.5	60
2	500	27.5	1.5	60
	500	27.5	1.5	75
4	950	27.5	2	72.1
5	500	30	1.5	60
6	500	27.5	1.5	50.2
7	800	5	2	94.716
8	500	27.5	1.5	60
9	800	24.5	1	94.21
10	500	27.5	1.5	60
11	950	27.5	3	60
12	800	25.3	2	93.824
13	200	5	2	30.1
14	950	50	1	90.10
15	800	50	1.5	93.719
16	200	5	1	31
17	950	27.5	3	55
18	200	50	1	30
19	800	5	2	93.1
20	950	27.5	2.3409	60

The Color value (whiteness) of the pigment was alnlyesized at low concteration ratio of titanium oxy-sulfet to urea molar ratio and at optiumam calcanation temperature and time.

The actual and predictive model in terms of coded and actual factors is presented below. This terms can be used to regenerate the results of this experiment, but they can not be used for modeling future response.

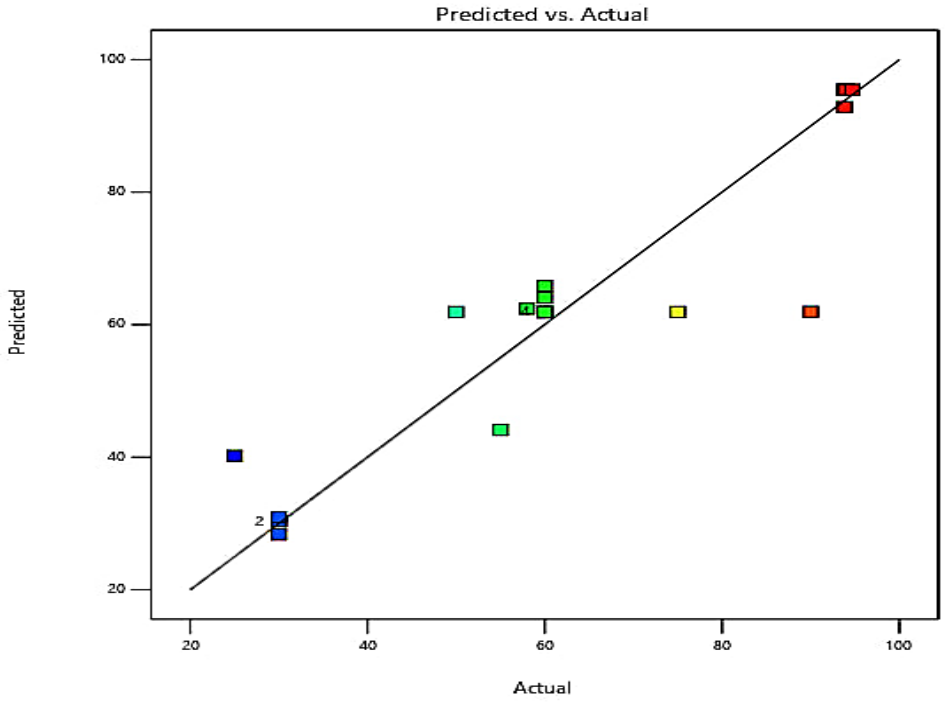

Figure 4.8: Diagnostic plot for the fitted model

Final Equation in Terms of Coded Factors:

Color value (whiteness) = +61.9047 + 32.5529 * A + 0.305374 * B + 1.30947 * C

Final equation interms of actual factors:

Color value (whiteness) = 3.34818 + 0.10851 *temperture + 0.0135722 * concenteration + 2.61893 * time

The relationships between the three factors are shown in Figure 4.9. Each plot shows the effects of two variables within their studied ranges, with the other variable fixed to the zero level. The response surface better visualizes the tendency of each factor to influence temperature and concretion on the sample. The shape of the response surface and contour plot shows the interaction of the three factors. (Q. Zhao et al)An elliptical contour plot indicates a prominent interaction, whereas a negligible effect appears as a circular contour plot.

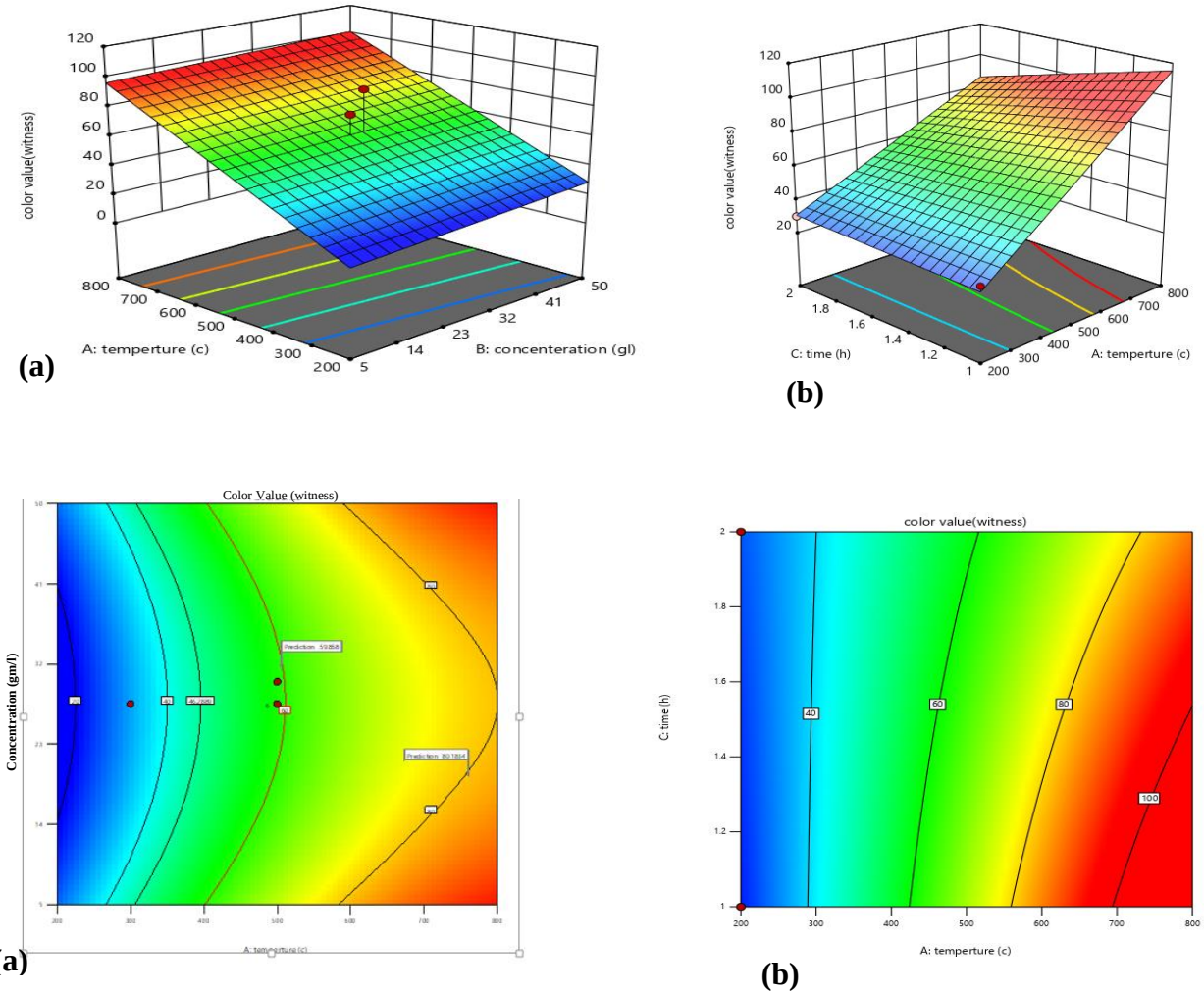

Figure 4.9: Effect of three parameters (temperature, concentration and time) on alpha alumina/tatania pigment (a) response surface and (b) contour plot of the experiment of Color value.

4.5 Condition optimization and confirmation test

The optimal conditions to obtain the high optical quality pearlescent pigment are confirmed according to the RSM under the optimal conditions. The temperature 800^0c for 2hr and the concentration selected 5gm/l. To confirm the validity of the experiment optimal response, three additional experiments were carried out under the optimal conditions. These results indicate that RSM is a very effective and powerful tool for optimization.

4.6 Performance analysis of synthesized pigment

To investigate the optical properties of the pigments, the pigment powders were pressed into a wafer with a diameter of 1.5 mm. Then, the spectral reflectance and the CIE L*a*b* of the pigment samples under 10°were measured by the UV-Vis spectrophotometer (D65 illuminant).

The optical quality of three sample result are the rutile fraction is at visible region (350-700 wave length) and this shows high reflectance of rutile phase is investigated. The percent reflectance and lightness value (L*) of the sample synthesized at lower urea concentration (more acidic environment) are better than others. Figure 4.10 shows the reflectance of the Alumina/titanium pigments with varying pH condition are Cleary shows a high reflectance in the whole visible region, so it has a white color. In order to further investigate the color characteristics of the pigments, CIE L*a*b* values of the pigment samples are measured.

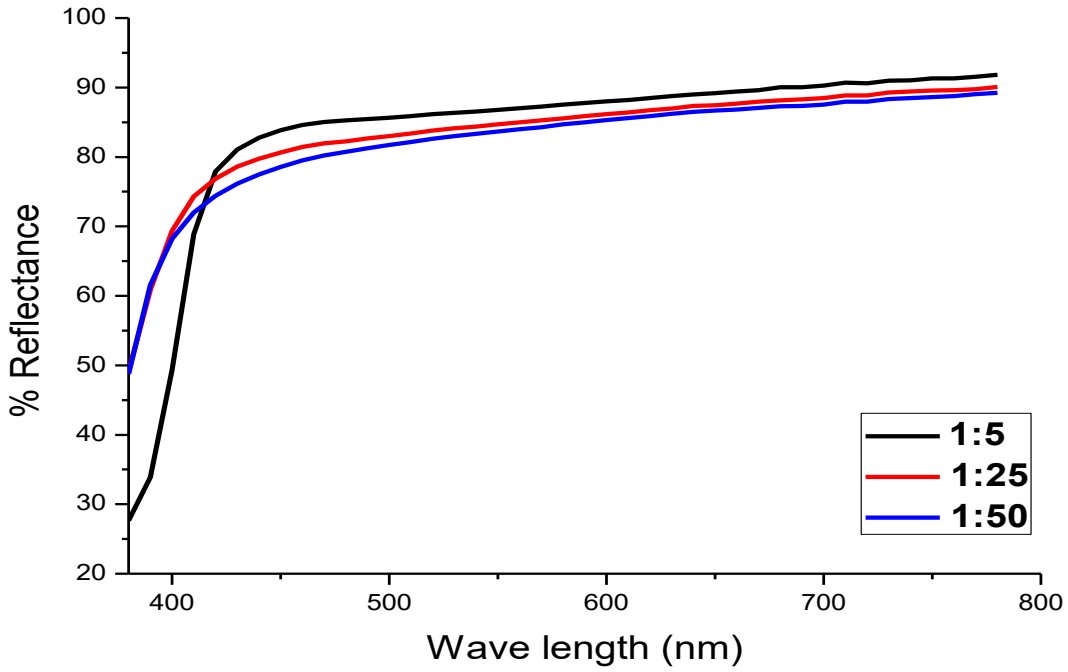

Fig 4.10: The spectral reflectance curves of Alumina/titania pigments with different pH conditions: (a) 1.5 (b) 1.25 (c) 1.50

4.7 Color characteristics of the samples

Ther optical property of the pigment which was assessed is the color value. The color values of the samples are measeured using colorimeters at the cental laboratory of KAIST. As can be seen from Table 4.7, the lightness value of the pigment with higher rutile phase fraction is higher than those with lower rutile phase fractions. The result is consistent with the values obtanined from the UV-Vis/NRI spectrophotometer. Scince rutile has higher refractive index it is more white than Anatase; thus, sample with higher rutile fraction has a higher degree of whitness than those with lower rutile phase fractions.

Table 4: 7: Lightness results of samples

Color coordinate					
Dilution	**Lightness value index**				
	Trial 1(L*value)	Trial 2(L*value)	Trial 3(L*value)	Average	Standard deviation
1:5	94.78	94.68	94.7311	94.73	0.040825
1:25	93.87	93.77	93.821	93.82	0.040828
1:50	93.367	93.371	93.4	93.37	0.014704

Values are mean ±SD, the difference of each sample are statistically significant difference (P<0.05).

As the result showes beter refractive index of rutile phase investegated .this result is found without usinge any titani diracting substreat .color value and the refactance angel is more better than other findings (Gao et al., 2012) and (Topuz et al., 2011).

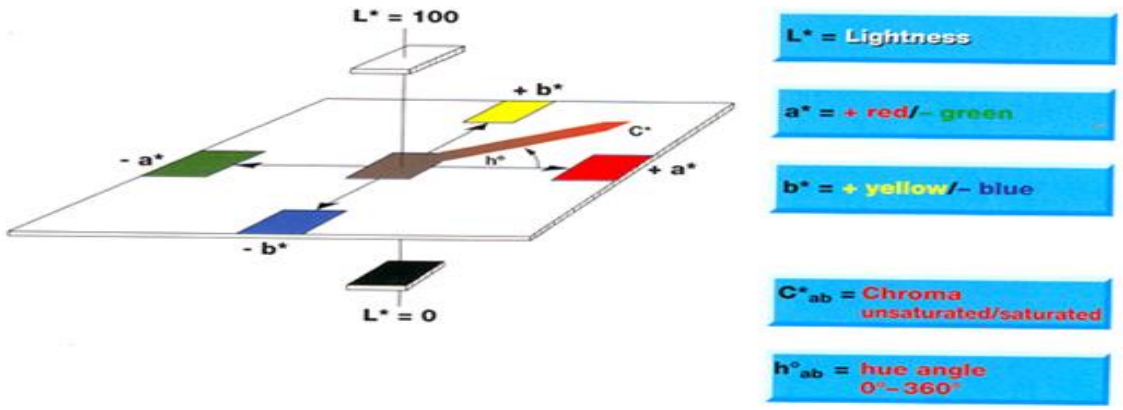

Fig 4.11: Color characteristics of the samples

5. CONCLUSION AND RECOMMENDATION

5.1 Conclusion

Pearlescent pigments were synthesized by coating α-alumina flakes with a thin layer of TiO_2. From the SEM images, the synthesized α-alumina nanoparticles are flaky shaped with smooth surface. α-alumina nanoparticles have better surface smoothness than the commercial mica. Coating of TiO_2 on the surface of the synthesized α-Al_2O_3 have been done using co-precipitation technique. Titanium oxy-sulfate has been used as a precursor. The hydrolysis of oxysulfate is highly affected by pH of the synthesis media. Ammonia obtained from in situ urea decomposition has been used to control the pH of the synthesis media. The pH is controlled by varying the ratio of urea to oxysulfate (1:5, 1:25 and 1:50). The sample with lower oxysulfate:urea ratio (i.e. strongly acidic synthesis media) resulted in higher rutile fraction (41.5%) while the other two samples, where the oxysulfate:urea ratios are 1:25 (i.e. close to neutral pH) and 1:50 (i.e. strongly basic synthesis media), resulted in extremely lower rutile phase fraction, 2.9% and 1.4% respectively. high rutile phase fraction coating after calcination with relatively low temperature at 800^0C for short period of heating time 2h. The morphology and the anatase-rutile transformation were studied by SEM and X-ray diffraction analysis As the result showes beter refractive index of rutile phase investegated . From the study the optical quality of three sample result are the rutile fraction is at visible region and this shows high reflectance of rutile phase is investigated. The percent of reflectance and lightness value (L*) of the sample synthesized at lower urea concentration (more acidic environment) better clor value and the refactance angel .this study result is found without usinge any titani diracting substreat .

5.2 Recommendation

5.2.1 Recommendations from this Study

According to this study, the alpha alumina substrate has higher surface smoothness than other natural and synthetic substrates and has high thermal and chemical stability; as well as high mechanical strength. This facilitates the coating of titanium oxide from low to high calcination temperature and reduces thermal expansion coefficient mismatch in the coting process .Using this coting mechanism for industrial producer of the pearlescent pigment. Better to reduce the cracking formation and degradation of the optical quality of pigment at high thermal stress is applied. Those industrial coatings and automobile paints industries use pearlescent pigments for both practical and ornamental purposes recommended based on this findings. Based on the findings of this study, the following recommendations are made:

1. In the pearlescent pigment production industries select the right substrate that helps to get high refractive index pigment in the pigment production.
2. Use nano-size flakes for the synthesis process, in this case the titanium oxide on alpha-alumina to achieve a luster pearl effect.
3. Produce the titanium (rutile) at low pH Value (acidic media) because the versions of pH have their impact on the formation of rutile-based TiO_2/pearlescent pigment.

5.2.1 Recommendations for Further Study

The use of pearlescent pigment is used in numerous industries today and has a high impact on the market. Synthesizing of high optical quality pearlescent pigment is vital to get the aesthetical property of the pigment. Standing from this work, the following recommendations are made for the study and future work

1. Raman spectroscopy analysis is better in revealing short term ordering.
2. More research should be done on Pilot scale production of the pigment
3. Testing the pigment in paints, cosmetics and plastics for better investigation

REFERENCES

Bayat, N., Baghshahi, S., & Alizadeh, P. (2008). Synthesis of white pearlescent pigments using the surface response method of statistical analysis. *Ceramics International*, *34*(8), 2029–2035. https://doi.org/10.1016/j.ceramint.2007.07.034

Byrne, C., Moran, L., Hermosilla, D., Merayo, N., Blanco, Á., Rhatigan, S., Hinder, S., Ganguly, P., Nolan, M., & Pillai, S. C. (2019). Effect of Cu doping on the anatase-to-rutile phase transition in TiO2 photocatalysts: Theory and experiments. *Applied Catalysis B: Environmental*, *246*, 266–276. https://doi.org/10.1016/j.apcatb.2019.01.058

Chamoli, S., Sharma, M., & Chamoli, M. A. (2021). *Organic Paints and Pigments : A Sustainable Approach*. *18*(3), 1071–1082. https://doi.org/10.29121/WEB/V18I3/12

Du, H., Liu, C., Sun, J., & Chen, Q. (2008). An investigation of angle-dependent optical properties of multi-layer structure pigments formed by metal-oxide-coated mica. *Powder Technology*, *185*(3), 291–296. https://doi.org/10.1016/j.powtec.2007.10.031

Fatimah, S., Ragadhita, R., Fitria, D., Husaeni, A., Bayu, A., & Nandiyanto, D. (2022). ASEAN Journal of Science and Engineering How to Calculate Crystallite Size from X-Ray Diffraction (XRD) using Scherrer Method. *Journal of Science and Engineering*, *2*(1), 65–76.

Gao, Q., Wu, X., Fan, Y., & Zhou, X. (2012). Low temperature synthesis and characterization of rutile TiO 2-coated mica-titania pigments. *Dyes and Pigments*, *95*(3), 534–539. https://doi.org/10.1016/j.dyepig.2012.06.006

Grosfils, P., & Lutsko, J. F. (2021). *Impact of Surface Roughness on Crystal Nucleation*.

Grzmil, B. U., Grela, D., & Kic, B. (2014). *Hydrolysis of titanium sulphate compounds Hydrolysis of titanium sulphate compounds ‡*. *February 2008*, 17–25. https://doi.org/10.2478/s11696-007-0074-8

Grzybowski, A., & Kupidura-Majewski, K. (2019). What is color and how it is perceived? *Clinics in Dermatology*, *37*(5), 392–401. https://doi.org/10.1016/j.clindermatol.2019.07.008

Horn, M., Schwerdtfeger, C. F., & Meagher, E. P. (1972). Refinement of the structure of anatase at several temperatures. *Zeitschrift Fur Kristallographie - New Crystal Structures*, *136*(3–4), 273–281.

https://doi.org/10.1524/zkri.1972.136.3-4.273

Hyoung, G. L., & Zuo, J. M. (2004). Growth and Phase Transformation of Nanometer-Sized Titanium Oxide Powders Produced by the Precipitation Method. *Journal of the American Ceramic Society*, *87*(3), 473–479. https://doi.org/10.1111/j.1551-2916.2004.00473.x

Ibrahim, S. A., & Sreekantan, S. (2011). Effect of pH on TiO2 nanoparticles via sol-gel method. *Advanced Materials Research*, *173*, 184–189. https://doi.org/10.4028/www.scientific.net/AMR.173.184

Islam, S., Rahman, R. A., Riaz, S., Naseem, S., & Ottoman, Z. (2015). Formation of Rutile Titania Phase at Low Temperature. In *Materials Today: Proceedings* (Vol. 2, Issue 10). Elsevier Ltd. https://doi.org/10.1016/j.matpr.2015.11.039

Li-Hui, Z., & Qing-Wei, H. (2011). Morphology control of α-Al2O3 platelets by molten salt synthesis. *Ceramics International*, *37*(1), 249–255. https://doi.org/10.1016/j.ceramint.2010.09.021

Maile, F. J., Pfaff, G., & Reynders, P. (2005). Effect pigments - Past, present and future. *Progress in Organic Coatings*, *54*(3), 150–163. https://doi.org/10.1016/j.porgcoat.2005.07.003

Mazzella, F. (2007). *An Overview : Composition , Optics and Uses*.

Mirhabibi, A. R. (2014). *Ceramic Coatings for Pigments*. *February 2012*. https://doi.org/10.5772/30010

Mohammed, A. A., Khodair, Z. T., & Khadom, A. A. (2020). Preparation and investigation of the structural properties of α-Al2O3 nanoparticles using the sol-gel method. *Chemical Data Collections*, *29*, 100531. https://doi.org/10.1016/j.cdc.2020.100531

Özer, N. (1992). Reproducibility of the coloration processes in TiO2 films. *Thin Solid Films*, *214*(1), 17–24. https://doi.org/10.1016/0040-6090(92)90450-P

Prorokova, N., Kumeeva, T., & Kholodkov, I. (2020). Formation of coatings based on titanium dioxide nanosolson polyester fibre materials. *Coatings*, *10*(1), 1–14. https://doi.org/10.3390/coatings10010082

Shindy, H. A. (2016). Basics in colors, dyes and pigments chemistry: a review. *Chemistry International* , *2*(1), 29–36.

Štengl, V., Šubrt, J., Bakardjieva, S., Kalendova, A., & Kalenda, P. (2003). The preparation and characteristics of

pigments based on mica coated with metal oxides. *Dyes and Pigments*, *58*(3), 239–244. https://doi.org/10.1016/S0143-7208(03)00086-X

Suyati, L., Fadilah Nur, I. D., Widodo, D. S., Gunawan, & Rahmanto, W. H. (2019). Electrosynthesis of Al(OH)3 by Al(s)|KCl(aq)||KCl(s)|C(s) system. *IOP Conference Series: Materials Science and Engineering*, *509*(1). https://doi.org/10.1088/1757-899X/509/1/012066

Tohidifar, M. R., Taheri-Nassaj, E., & Alizadeh, P. (2008). Optimization of the synthesis of a nano-sized mica-hematite pearlescent pigment. *Materials Chemistry and Physics*, *109*(1), 137–142. https://doi.org/10.1016/j.matchemphys.2007.11.004

Topuz, B. B., Gündüz, G., Mavis, B., & Çolak, Ü. (2011). The effect of tin dioxide (SnO2) on the anatase-rutile phase transformation of titania (TiO2) in mica-titania pigments and their use in paint. *Dyes and Pigments*, *90*(2), 123–128. https://doi.org/10.1016/j.dyepig.2010.12.013

Zhang, X., Wang, L., Hu, W., Zheng, H., & Zhang, X. (2018). The synthesis of titanium dioxide nanoparticles from titanium slag and its use for low temperature SCR catalyst. *IOP Conference Series: Earth and Environmental Science*, *208*(1). https://doi.org/10.1088/1755-1315/208/1/012011

Allen NS et al. (2004). Degradation and stabilisation of polymers and coatings: nano versus pigmentary titania particles. *Polym Degrad Stab*, 85(3):927-46.

B.-Z. Lin and S.-X. Liu, . (1999). Acta Crystallogr. Cryst.Struct. Commun., . , Sect. C:, 55, 1961–1963.

D. T. Cromer and K. Herrington. (1955). *J. Am. Chem. Soc.*, 77, 4708-4709.

R.Song et al. (2005). Preparation and phase transformation of anatase rutile crystals in metal-doped TiO2/muscovite nanocomposites. *Thin Solid Films.*, 491(1-2):110-6.

Wu J-M, Qi B. . (2008). Low-temperature growth of rutile nanorod thin films and their photon-induced property. *J Am Ceram Soc*, 91(12):3961-70.

Zhang S et al. (2009). Room temperature synthesis of nearly monodisperse rodlike rutile TiO2 nanocrystals. *Mater Lett* , 63(1):127-9.Arunachalam et al. (2011). *Sci. Technol.*, 4, 65 .

Bayat N, Baghshahi S, Alizadeh P. (2008). Synthesis of white pearlescent pigments using the surface response method of statistical analysis. *Ceram Int*, 34(8):2029-35.

Bertaux S et al. (2005). *Thin Solid Films* , 473(1):80-8.

C. Aprile, A. Corma and H. Garcia. (2008). *Phys. Chem. Chem. Phys.*, 10, 769-783.

Cavalcante PMT et al. (2007). Ceramic application of mica titania pearlescent pigments. Dyes Pigm. ;74(1):1-8.

Cho JH et al. (2009). Room-temperature synthesis and characteristics of nanocrystalline TiO2 on mica by homogeneous precipitation. *Met Mater Int*, 15(6):1001-5.

D. Makow,et al. (1985). 123,347.

Eskelinen P et al. (1993). The effect of calcination on the surface omposition and structure of titanium dioxide coated mica particles. *J Solid State Chem* ., 103(1):160-9.

G. Pfaff, P. R. ((1999) 1963). *Reynders, Chem.99*.

Ge M et al. (2011). Template-free synthesis and photocatalytic application of rutile TiO2 hierarchical nanostructures. *Ind Eng Chem Res*, 50(11):6681-7.

Gemdat G. (2017). "Pearl". .*Archived from the original*.

H. Cheng, J. a. (1995). *Chem. Mater.*, 7, 663-671.

H. Zhang and J. F. Banfield. (2000). *Mater. Res.*,, 15, 437-448.

H. Zhang, and J. F. Banfield. (1999). *Am. Mineral.*, 84, 528-535.

Holleman, A. F. et al. (2001). Inorganic Chemistry",. *Academic Press: San Diego ISBN 0-12-352651-5.*

J. L. Look and C. F. Zukoski. (1992). *J. Am. Ceram. Soc.*, , 75, 1587-1595.

J. Livage, M. Henry and C. Sanchez, . (1988). *Prog. Solid State Chem.*, , 18, 259-341.

J. Tan, L. e. ((2004)). Dyes Pigments 62. 107.

Joglekar et al. (1987). Product Excellence through Design of Experiments. *Cereal Foods World*, , 32, 857-868.

K. Nitta, e. a. (1997). *European Patent Application* , 763,573 .

L. Sung, et al. (2000). Polymeric Materials. *Science and Engineering (PMSE)*, p. 343.

L.M. Greenstein, i. P. (1998). New York,: Lewis (Ed.), Pigment Handbook, vol. I,second ed., John Wiley & Sons, p. 829.

M. Gopal, et al. (1997). *Mater. Sci.*, ,32, 6001-6008.

M. Levlin, et al. ((2001). *Sic,*, 171,257.

M. Ren et al. . (2007). Materials Chemistry and Physics. 103 ,230–234.

M.A. Barakat et al. (2005). Nanotechnol. . 5 , 759.

N.G. Semaltianos. (2000). Thin Solid Films. *E.G. Wilson,*, 366 , 111.

Pfaff et al. (1998). Encyclopedia of Industrial Chemistry:. In *Pigments, Inorganic, Section 4.3*, (pp. , sixth ed., VCH Verlagsgesellschaft,). , Germany: Weinheim(electronic release).

Pfaff G, Reynders P. (1999). Angle-dependent optical effects deriving from submicron structures of films and pigments. *Chem Rev* , ;99(7):1963-82.

Podszus E. (1923). Hartstoff-Metall AG,. *GB Patent, 204,055*.

Q. Zhao et al. (n.d.). *Hazard. Mater.*, 144, 499 (2007).

R. L. Penn and J. F. Banfield. (1998). *Am. Mineral.*, 83, 1077-1082.

R. L. Penn and J. F. Banfield. (1998). *Am. Mineral.*, , 83, 1077-1082.

R. L. Penn and J. F. Banfield. (1999). , *Am. Mineral.*, , , 84, 871-876.

S. M. Gupta and M. Tripathi. (2012). *Cent. Eur. J. Chem.*,, 10, 279-294;.

V. Stengl et al. (2003). Dyes Pigments. 58, 239.

Wiley-VCH, P. G. (n.d.).

X. Chen and S. S. Mao. (2007). *Chem. Rev.*,, 107, 2891-2959.

X. Lang, X. Chen and J. Zhao. (2014). *Chem. Soc. Rev.*,, , 43, 473-486;.

Y. Hu, et al. (2003). *Mater. Sci. Eng. A*, , 344, 209-214.

Y. Li, T. J. White and S. H. Lim, J. (2004). *Solid State Chem*, 177, 1372-1381.

Y. Liao, et al.. *J. Mater. Chem.*, , 22 (2012)

Y. Yoshizawa et al. (1998). Preparation of high fracture toughness alumina sintered bodies from bayer aluminum hydroxide. *Journal of the Ceramic Society of Japan 106 (12)*, (1998)1172–1177.

APPENDIX

In this work, the most important factors, three of them, i.e. the solution concentration, temperature, and time were studied (Table 1).

To study the effect of these factors, a statistical method of design of experiments named as ‘‘response surface method’’ (RSM) in a ‘‘face-centered composite’’ was used. As seen in Table 1, the factors were studied at three levels. Hence, according to the face-centered composite, twenty experiments were conducted. The concentration of which is given in Tables 1 and 2.The temperature of the solutions was adjusted

Table 1: the levels used for concentration, temperature and time

Factor		Level		
		1	0	-1
X1	Concentration (gl^{-1})	5	25	50
X2	Temperature (°C)	200	500	950
X3	Time (h)	1	2	3

- **Model Comparison Statistics**

Table 2: Comparison Statistics

PRESS	3.547E+05
-2 Log Likelihood	138.77
BIC	165.73
AICc	174.77

- **Coefficients in Terms of Coded Factors**

Table 3: Coded Factors

Factor	Coefficient Estimate	df	Standard Error	95% CI Low	95% CI High	VIF
Intercept	63.71	1	3.85	55.23	72.18	
A-temperature	31.86	1	7.81	14.66	49.06	4.90
B-concentration	-1.35	1	6.53	-15.74	13.03	4.12
C-time	-1.87	1	3.43	-9.41	5.67	2.35
AB	-14.37	1	11.26	-39.16	10.41	8.32
AC	-13.25	1	8.03	-30.92	4.43	6.93
BC	-13.84	1	9.80	-35.41	7.72	6.30
A^2	-16.99	1	13.05	-45.70	11.73	6.89
A^2C	1.52	1	5.87	-11.40	14.44	2.62

When all other factors are maintained constant, the coefficient estimate shows the expected change in response for each unit change in factor value. The total average response of all the runs is the intercept in an orthogonal design. Based on the factor choices, the coefficients represent modifications made around that average. VIFs are 1 when the factors are orthogonal; VIFs more than 1 denote multi-collinearity; the higher the VIF, the stronger the factor connection. VIFs of fewer than 10 are generally acceptable.

- **Final Equation in Terms of Coded Factors**

Table 4: Final Equation in Terms of Coded Factors

color value(witness)	=
+63.71	
+31.86	*A
-1.35	*B
-1.87	*C
-14.37	*AB
-13.25	*AC
-13.84	*BC
-16.99	*A^2
+1.52	*A^2C

It is possible to predict the reaction for specific levels of each element by using the equation expressed in terms of coded factors. The factors' high levels are automatically written as +1 and their low levels as -1. By comparing the factor coefficients, the coded equation can be used to determine the relative impact of the components.

- **Final Equation in Terms of Actual Factors**

  Table 5: Final Equation in Terms of Actual Factors

color value(witness)	=
-188.25494	
+0.536639	Temperature
+2.85005	Concentration
+82.70162	Time
-0.002129	temperature * concentration
-0.122086	temperature * time
-1.23049	concentration * time
-0.000239	temperture^2
+0.000034	temperture^2 * time

Predictions on the response for specific levels of each factor can be made using the equation expressed in terms of the actual factors. In this case, each factor's levels ought to be stated in their original units. Because the intercept is not in the middle of the design space and the coefficients are scaled to account for the units of each element, this equation should not be used to calculate the relative influence of each factor.

Coefficients in Terms of Coded Factors

Table 6: Coefficient of coded factors

Factor	Coefficient Estimate	df	Standard Error	95% CI Low	95% CI High	VIF
Intercept	61.90	1	2.52	56.55	67.26	
A-temperature	32.55	1	3.73	24.64	40.47	1.27
B-concentration	0.3054	1	3.44	-6.99	7.60	1.30
C-time	1.31	1	2.17	-3.28	5.90	1.07

The coefficient estimate, assuming that all other factors remain constant, shows the anticipated change in response for each unit change in factor value. The average reaction over all runs in an orthogonal design is called the intercept. Depending on the factor parameters, the coefficients are modifications made to that average. A VIF of one indicates that the factors are orthogonal; VIFs larger than one signify multi-colinearity; the higher the VIF, the more severe the factor correlation. Generally speaking, VIFs under 10 are acceptable.

- **Fit Summary**

Table 7: R^2 value

Source	Sequential p-value	Lack of Fit p-value	Adjusted R^2	Predicted R^2	
Linear	< 0.0001	0.0381	0.8288	0.8097	Suggested
2FI	0.7075	0.0188	0.8100	0.6350	
Quadratic	0.0934	0.0328	0.8662	-2.5548	
Cubic	0.0328		0.9288		Aliased

- **Sequential Model Sum of Squares**

Table 8: Model Sum of Squares

Source	Sum of Squares	Df	Mean Square	F-value	p-value	
Mean vs Total	73121.85	1	73121.85			
Linear vs Mean	9175.28	3	3058.43	31.67	< 0.0001	Suggested
2FI vs Linear	151.55	3	50.52	0.4712	0.7075	
Quadratic vs 2FI	638.61	3	212.87	2.82	0.0934	
Cubic vs Quadratic	433.75	2	216.88	5.40	0.0328	Aliased
Residual	321.31	8	40.16			
Total	83842.36	20	4192.12			

- **Factors**

Table 9: Point of prediction

Factor	Name	Level	Low level	High level	Std.Dev.	Coding
A	Temperature	800.00	200.00	800.00	0.0000	Actual
B	concentration	5.00	5.00	50.00	0.0000	Actual
C	Time	2.00	1.0000	2.00	0.0000	Actual

- **Confirmation Location #1**

Table 10: Optimization conformation location

Temperature	Concentration	Time
800	5	2

- **Confirmation**

Table 11: Two-sided Confidence = 95%

Analysis	Predicted Mean	Predicted Median	observed	Std Dev	SE Mean	95%CI low for Mean	95%CI high for Mean	95%TI low for99% Pop	95%TI high for99% Pop
Color value(witness) test(1)	95.4617	95.4617		9.82737	4.45015	86.028	104.896	51.8073	139.116
value(witness) (4)	95.4617	95.4617		9.82737	4.45015	86.028	104.896	51.8073	139.116
value(witness) (7)	95.4617	95.4617		9.82737	4.45015	86.028	104.896	51.8073	139.116

- Report

Table 12: Comparison of predicted and experimental tested data

Run Order	Actual Value	Predicted Value	Residual	Leverage	Internally Studentized Residuals	Externally Studentized Residuals	Cook's Distance	Influence on Fitted Value DFFITS	Standard Order
1	60.00	61.09	-1.09	0.095	-0.111	-0.107	0.000	-0.034	19
2	60.00	61.09	-1.09	0.095	-0.111	-0.107	0.000	-0.034	17
3	75.00	61.09	13.91	0.095	1.412	1.474	0.030	0.477	16
4	25.00	36.11	-11.11	0.250	-1.239	-1.267	0.073	-0.731	9
5	90.00	61.51	28.49	0.096	2.895	4.666(1)	0.128	1.524	11
6	50.00	61.09	-11.09	0.095	-1.126	-1.139	0.019	-0.369	20
7	94.00	95.03	-1.03	0.305	-0.120	-0.115	0.001	-0.076	6
8	60.00	61.09	-1.09	0.095	-0.111	-0.107	0.000	-0.034	18
9	93.78	95.03	-1.26	0.305	-0.145	-0.140	0.001	-0.093	2
10	60.00	61.09	-1.09	0.095	-0.111	-0.107	0.000	-0.034	15
11	60.00	61.34	-1.34	0.509	-0.184	-0.177	0.005	-0.181	13
12	94.72	95.03	-0.3172	0.305	-0.037	-0.035	0.000	-0.023	8
13	30.00	31.95	-1.95	0.422	-0.248	-0.238	0.006	-0.204	5
14	93.82	97.51	-3.69	0.773(2)	-0.749	-0.736	0.274	-1.359	4
15	58.00	67.37	-9.37	0.775(2)	-1.910	-2.164	1.799(3)	-4.020(3)	12
16	30.00	31.95	-1.95	0.422	-0.248	-0.238	0.006	-0.204	1
17	55.00	51.10	3.90	0.690	0.675	0.661	0.145	0.985	10
18	30.00	27.39	2.61	0.745(2)	0.498	0.483	0.104	0.826	3
19	30.00	30.20	-0.2014	0.636	-0.032	-0.031	0.000	-0.041	7
20	60.00	61.23	-1.23	0.196	-0.132	-0.127	0.001	-0.063	14

(1) Observation with |External Stud. Residuals| > 3.81

(2) Observation with leverage > 2.00 × (average leverage).

The model accuracy was checked by comparing the predicted and experimental value .the straight line means that no response transformation was required and that there was no apparent problem with normality

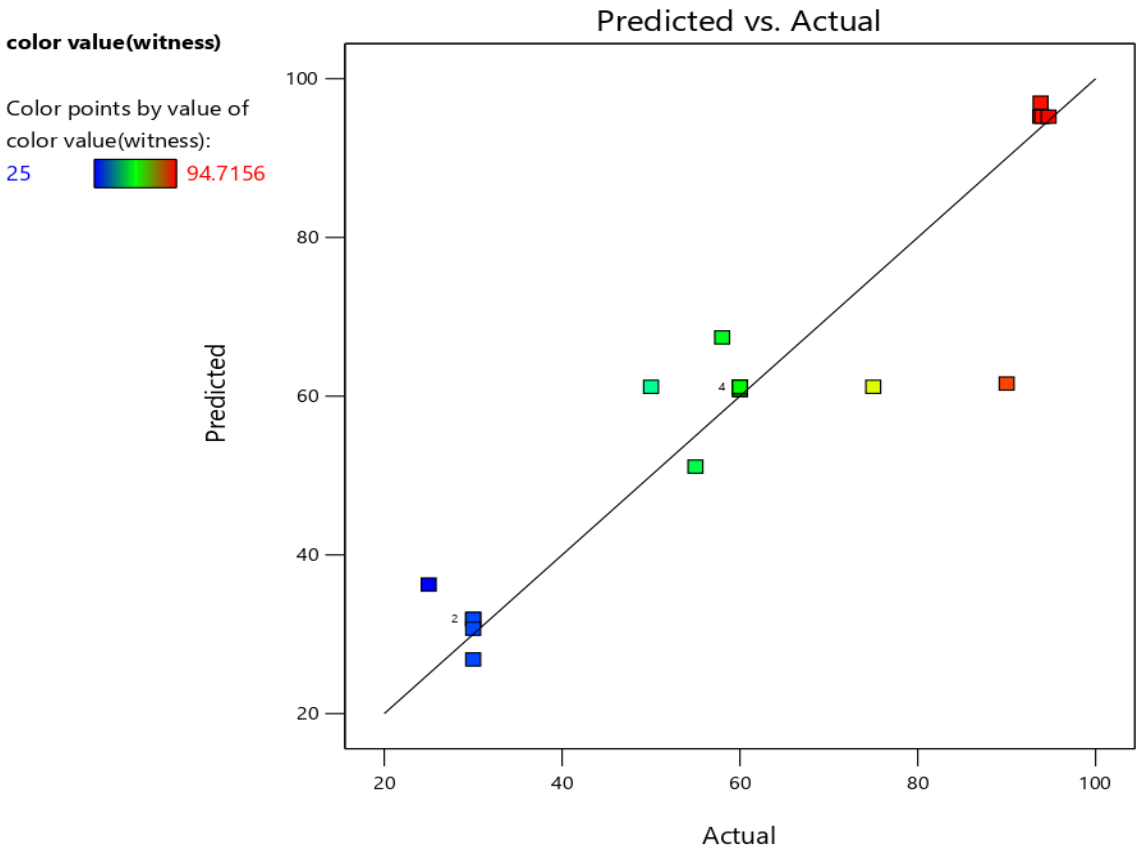

Figure 1.Comparison of predicted and experimental data plot

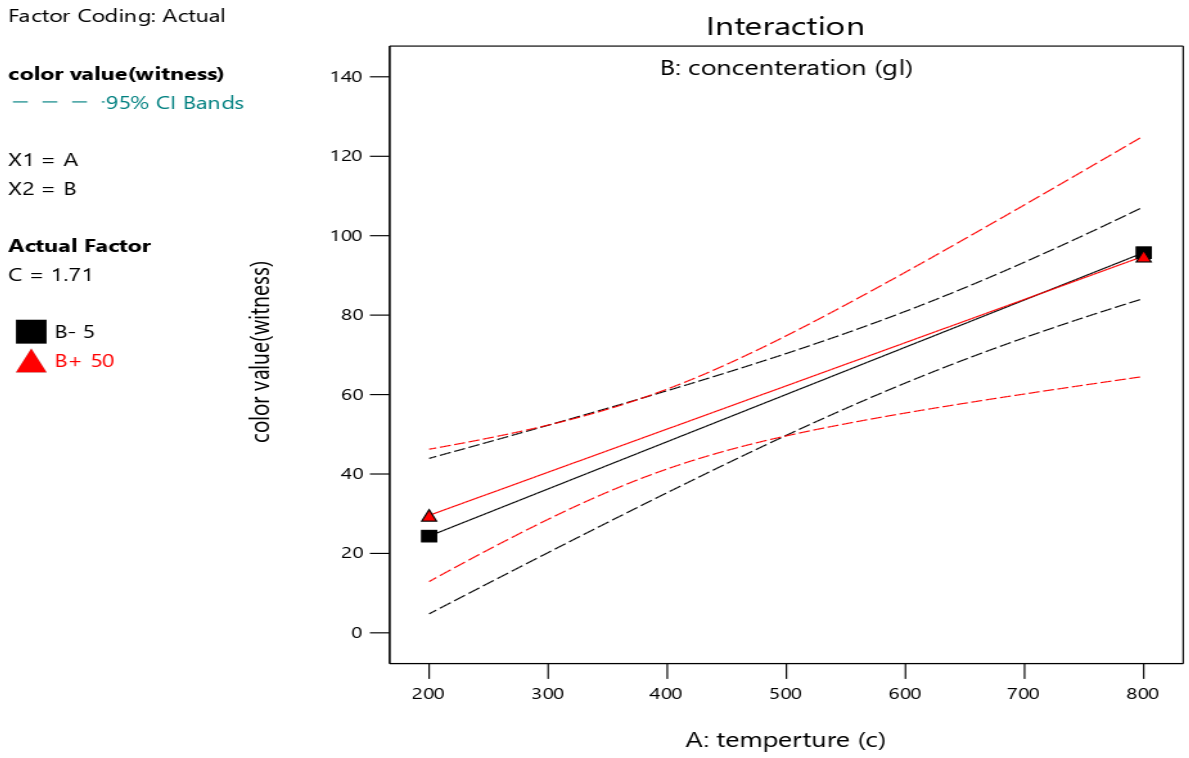

Figure 2.Comparison of plot of Surface interaction

Response surface analysis

Effect of the refraction depending on initial concentration of $TioSo_4$ urea ratio ,temperature and time have an impact on the color value .the surface response and contour plot shows as the calcination temperature increased with decreasing the concentration of reaction

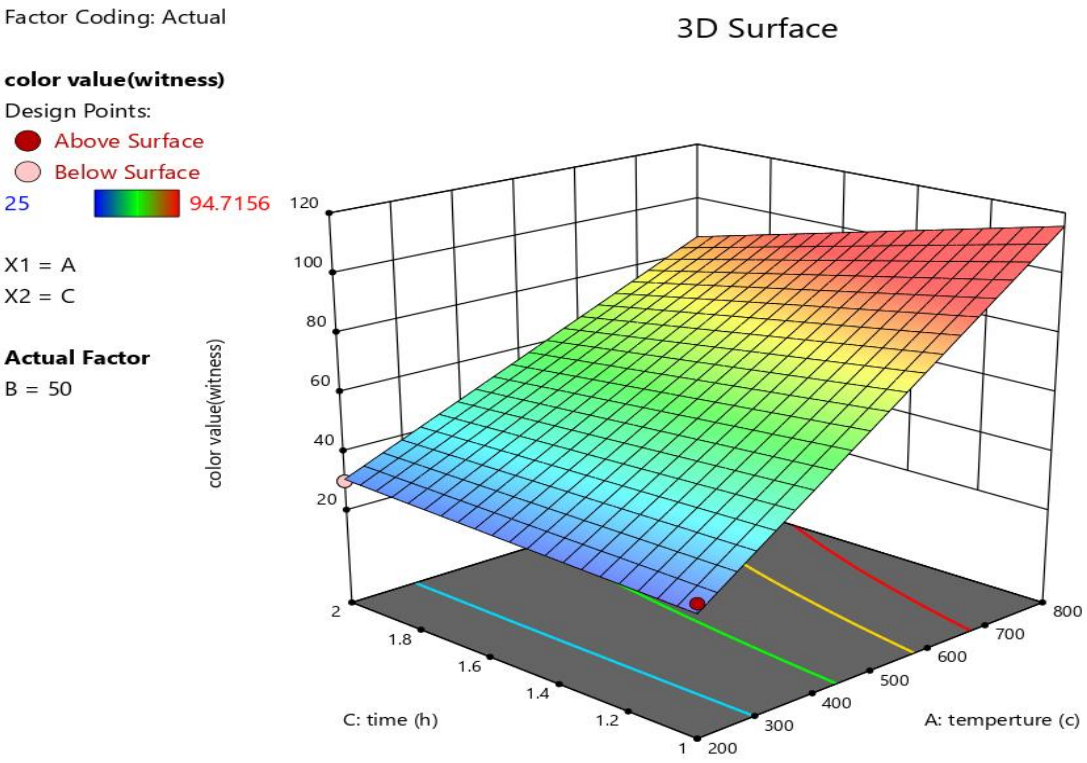

Figure 3: Effect of temperature and time on color value (witness) surface response plot

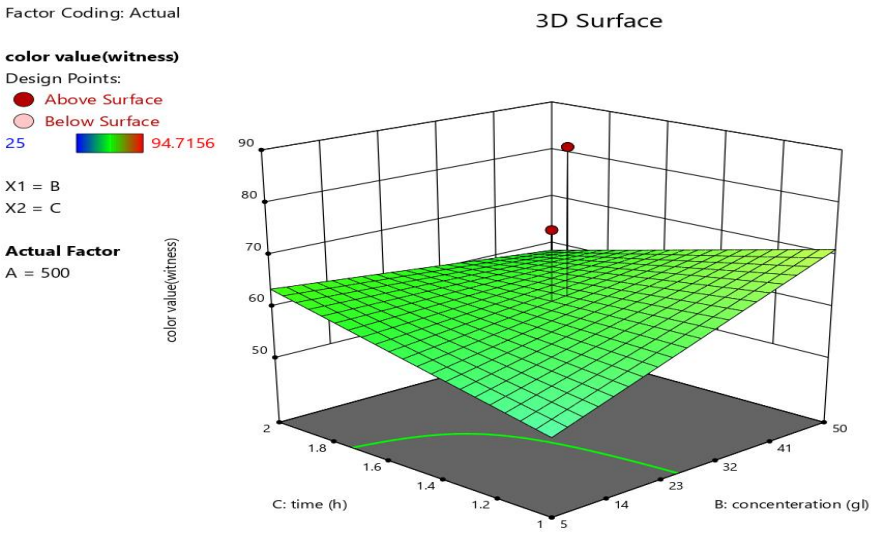

Figure 4: Effect of concentration and time on color value (witness) surface response plot

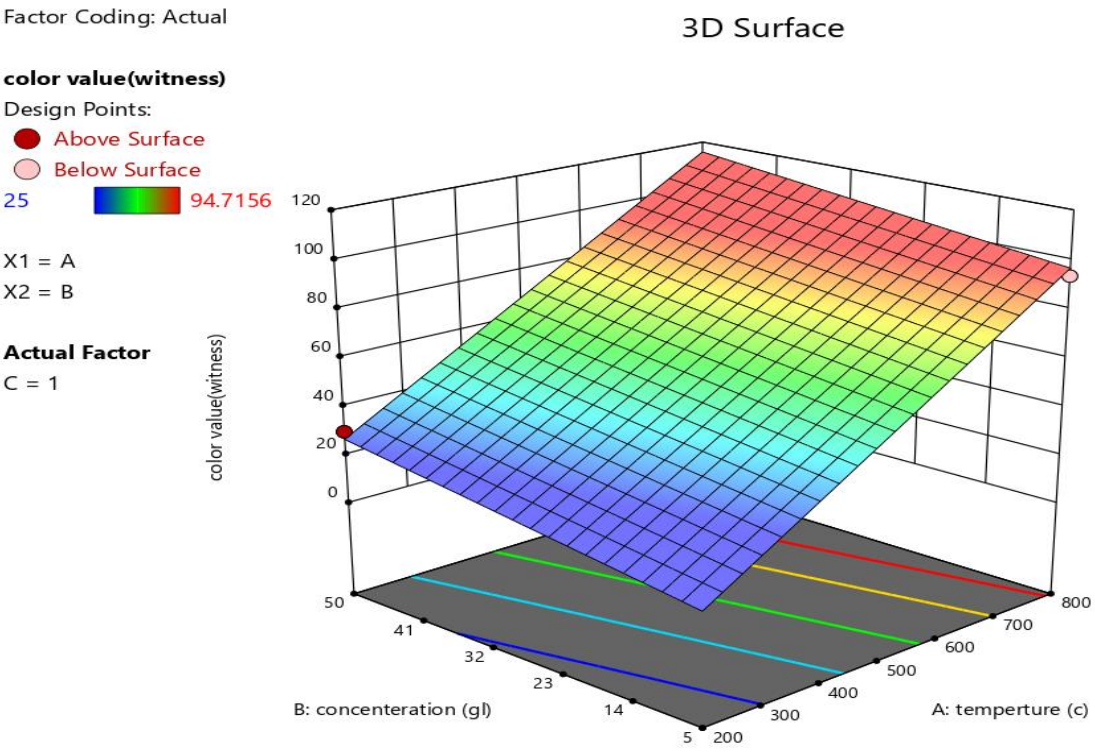

Figure 5: Effect of concentration and temperature on color value (witness) surface response plot